



DETERMINATION OF THE OPTIMAL LOCATION OF  
A 2-DOF MANIPULATOR FOR MINIMAL ENERGY  
CONSUMPTION DURING A PREDEFINED TASK

Mehmet Beşir KOPMAZ

Master of Science Thesis

Department of Mechatronics Engineering

Asst. Prof. Dr. İsmail BÜTÜN

2016



**T.R.**  
**BURSA TECHNICAL UNIVERSITY**  
**GRADUATE SCHOOL OF NATURAL AND APPLIED SCIENCES**

**DETERMINATION OF THE OPTIMAL LOCATION OF A 2-DOF  
MANIPULATOR FOR MINIMAL ENERGY CONSUMPTION DURING A  
PREDEFINED TASK**

**A THESIS FOR THE DEGREE OF MASTER OF SCIENCE**

**Mehmet Beşir KOPMAZ**

**Department of Mechatronics Engineering**

**Bursa**  
**March 2016**

## MASTER THESIS EXAMINATION RESULT FORM

The thesis entitled “Determination of the Optimal Location of a 2-DoF Manipulator for Minimal Energy Consumption During a Predefined Task” completed by Mehmet Beşir KOPMAZ under supervision of Asst. Prof. İsmail BÜTÜN has been reviewed in terms of scope and quality and approved as a thesis for the degree of Master of Science.

### Jury Members

Asst. Prof. İsmail BÜTÜN

(Bursa Technical University,

Department of Mechatronics Engineering) .....

Assoc. Prof. Hakan GÖKDAĞ

(Bursa Technical University,

Department of Mechanical Engineering) .....

Asst. Prof. Gürsel ŞEFKAT

(Uludağ University,

Department of Mechanical Engineering) .....

Date of Examination: 15/03/2016

Director of Graduate School of Natural and Applied Sciences

Prof. Nurettin ACIR

Date/Signature

## DECLARATION ON PLAGIARISM

I hereby declare that this piece of written work is the result of my own independent scholarly work, and that in all cases material from the work of others is acknowledged, and quotations and paraphrases are clearly indicated. No material other than listed has been used. I am aware of what constitutes an act of plagiarism and understand that my thesis will be rejected if found to contain any instance of plagiarism.

Student Name and Surname: Mehmet Beşir KOPMAZ

Signature:



## ACKNOWLEDGEMENTS

I would like to express my deepest gratitude to my advisor, Assistant Professor İsmail BÜTÜN. I have been amazingly fortunate to have an advisor who gave me the freedom to explore on my own, and at the same time the guidance to recover when my steps faltered. His patience and support helped me overcome many crisis situations and finish this thesis. I hope that one day I would become as good an advisor to my students as he has been to me.

My sincere gratitude is also to Professor Osman Kopmaz who has been always there to listen and give advice, encouraging me throughout this endeavor. I am deeply grateful to him for the long discussions that helped me sort out the technical details of my work. I am also thankful to him for encouraging the use of correct grammar and consistent notation in my writings and for carefully reading and commenting on countless revisions of this manuscript.

Most importantly, none of this would have been possible without the love and patience of my family, to whom this thesis is dedicated to. They have been a shelter for me in the confinement of humanity in this corner of the cosmos with their love, concern, support and optimism all these years; a chance to feel special, rather than to be crushed by the weight and beauty of our own loneliness.

**Mehmet Beşir KOPMAZ**

## TABLE OF CONTENTS

### Page No.

Outer Cover	
Inner Cover	
Master Thesis Examination Result Form	
Declaration on Plagiarism	
Acknowledgements	
Table of Contents	v
List of Figures	vi
List of Symbols	viii
Özet	xi
Abstract	xii
<b>1. INTRODUCTION</b>	<b>1</b>
<b>2. LITERATURE SEARCH</b>	<b>2</b>
<b>3. INVERSE ANALYSIS</b>	<b>5</b>
3.1. Position Analysis	6
3.2. Velocity Analysis	7
3.3. Acceleration Analysis	8
<b>4. DEFINITION OF TASK AND SEARCHING OPTIMAL TRAJECTORY</b>	<b>9</b>
<b>5. KINEMATIC CONSTRAINTS, VELOCITY AND ACCELERATION FUNCTIONS</b>	<b>15</b>
<b>6. EQUATIONS OF MOTION</b>	<b>16</b>
<b>7. SOLVING EQUATION OF MOTION FOR ACTUATOR TORQUES</b>	<b>21</b>
<b>8. CALCULATION OF ENERGY CONSUMPTION</b>	<b>22</b>
<b>9. NUMERICAL EXAMPLES</b>	<b>23</b>
<b>10. CONCLUSION</b>	<b>45</b>
<b>REFERENCES</b>	<b>46</b>
<b>RESUME</b>	<b>47</b>

## LIST OF FIGURES

<b>Figure 3.1</b> Manipulator of interest	5
<b>Figure 4.1</b> Geometric definition of trajectory	10
<b>Figure 4.2</b> The longest possible trajectory	11
<b>Figure 4.3</b> New coordinate system with respect to minimal energy trajectory	14
<b>Figure 9.1</b> Position angles of links in Example 1	25
<b>Figure 9.2</b> Angular velocities of links in Example 1	25
<b>Figure 9.3</b> Angular accelerations of links in Example 1	26
<b>Figure 9.4</b> Actuator torques of links in Example 1	26
<b>Figure 9.5</b> Actuator powers of links in Example 1	27
<b>Figure 9.6</b> Position angles of links in Example 2	28
<b>Figure 9.7</b> Angular velocities of links in Example 2	29
<b>Figure 9.8</b> Angular accelerations of links in Example 2	29
<b>Figure 9.9</b> Actuator torques of links in Example 2	30
<b>Figure 9.10</b> Actuator powers of links in Example 2	30
<b>Figure 9.11</b> Energy consumptions for both configurations in Example 2	31
<b>Figure 9.12</b> Position angles of links in Example 3	32
<b>Figure 9.13</b> Angular velocities of links in Example 3	33
<b>Figure 9.14</b> Angular accelerations of links in Example 3	33
<b>Figure 9.15</b> Actuator torques of links in Example 3	34
<b>Figure 9.16</b> Actuator powers of links in Example 3	34
<b>Figure 9.17</b> Energy consumptions for both configurations in Example 3	35
<b>Figure 9.18</b> Position angles of links in Example 4	36
<b>Figure 9.19</b> Angular velocities of links in Example 4	37
<b>Figure 9.20</b> Angular accelerations of links in Example 4	37
<b>Figure 9.21</b> Actuator torques of links in Example 4	38
<b>Figure 9.22</b> Actuator powers of links in Example 4	38
<b>Figure 9.23</b> Energy consumptions for both configurations in Example 4	39
<b>Figure 9.24</b> Position angles of links in Example 5	40
<b>Figure 9.25</b> Angular velocities of links in Example 5	41
<b>Figure 9.26</b> Angular accelerations of links in Example 5	41
<b>Figure 9.27</b> Actuator torques of links in Example 5	42
<b>Figure 9.28</b> Actuator powers of links in Example 5	42

**Figure 9.29** Energy consumptions for both configurations in Example 5 43

**Figure 9.30** The optimal loci of the root of manipulator in the XY coordinate system 44





## LIST OF SYMBOLS AND ACRONYMS

<b>Symbol</b>	<b>Definition</b>
$I_{1,O}$	Mass moment of inertia of link 1 with respect to point $O$
$I_{2,A}$	Mass moment of inertia of link 2 with respect to point $A$
$I_{G_1}$	Mass moment of inertia of link 1 with respect to point $G_1$
$I_{G_2}$	Mass moment of inertia of link 2 with respect to point $G_2$
$L$	Length of trajectory
$L_{max}$	Maximum possible length of trajectory
$L_1$	Length of link 1
$L_2$	Length of link 2
$\mathbf{M}_1$	Torque vector of actuator 1
$M_1$	Torque of actuator 1
$M_{11}$	Torque of actuator 1 for configuration 1
$M_{12}$	Torque of actuator 1 for configuration 2
$\mathbf{M}_2$	Torque vector of actuator 2
$M_2$	Torque of actuator 2
$M_{21}$	Torque of actuator 2 for configuration 1
$M_{22}$	Torque of actuator 2 for configuration 2
$P_1$	Power of actuator 1
$P_{11}$	Power of actuator 1 for configuration 1
$P_{12}$	Power of actuator 1 for configuration 2
$P_2$	Power of actuator 2
$P_{21}$	Power of actuator 2 for configuration 1
$P_{22}$	Power of actuator 2 for configuration 2
$T$	Total kinetic energy of manipulator
$T_1$	Kinetic energy of link 1
$T_2$	Kinetic energy of link 2
$T_m$	Kinetic energy of payload mass $m$

$W$	Total virtual work of actuator torques
$W_1$	Virtual work done on link 1
$W_2$	Virtual work done on link 2
$r_{G_1}$	Distance of center of gravity of link 1 from point $O$
$r_{G_2}$	Distance of center of gravity of link 2 from point $A$
$s(t)$	Motion program
$\dot{s}(t)$	First time derivative of motion program
$\ddot{s}(t)$	Second time derivative of motion program
$\mathbf{v}_A$	Velocity vector of point $A$
$\mathbf{v}_B$	Velocity vector of point $B$
$v_B$	Linear speed of point $B$
$\mathbf{v}_{B/A}$	Velocity vector of point $B$ with respect to point $A$
$\mathbf{v}_{G_1}$	Velocity vector of point $G_1$
$v_{G_1}$	Linear speed of point $G_1$
$\mathbf{v}_{G_2}$	Velocity vector of point $G_2$
$v_{G_2}$	Linear speed of point $G_2$
$\mathbf{v}_{G_2/A}$	Velocity vector of point $G_2$ with respect to point $A$
$\mathbf{u}$	Trajectory direction unit vector
$x$	Abscissa of a generic point on the trajectory
$\dot{x}$	$x$ -component of end point velocity
$\ddot{x}$	$x$ -component of end point acceleration
$x_F$	Abscissa of final point of trajectory
$x_S$	Abscissa of starting point of trajectory
$x_{S_{init}}$	Initial abscissa of starting point
$x_{S_{fin}}$	Final abscissa of starting point
$y$	Ordinate of a generic point on the trajectory
$\dot{y}$	$y$ -component of end point velocity
$\ddot{y}$	$y$ -component of end point acceleration

$y_F$	Ordinate of final point of trajectory
$y_S$	Ordinate of starting point of trajectory
$\theta_1$	Position angle of link 1
$\theta_{11}$	Position angle of link 1 for configuration 1
$\theta_{12}$	Position angle of link 1 for configuration 2
$\theta_2$	Position angle of link 2
$\theta_{21}$	Position angle of link 2 for configuration 1
$\theta_{22}$	Position angle of link 2 for configuration 2
$\dot{\theta}_1$	Angular speed of link 1
$\dot{\theta}_{11}$	Angular speed of link 1 for configuration 1
$\dot{\theta}_{12}$	Angular speed of link 1 for configuration 2
$\dot{\theta}_2$	Angular speed of link 2
$\dot{\theta}_{21}$	Angular speed of link 2 for configuration 1
$\dot{\theta}_{22}$	Angular speed of link 2 for configuration 2
$\ddot{\theta}_1$	Angular acceleration of link 1
$\ddot{\theta}_{11}$	Angular acceleration of link 1 for configuration 1
$\ddot{\theta}_{12}$	Angular acceleration of link 1 for configuration 2
$\ddot{\theta}_2$	Angular acceleration of link 2
$\ddot{\theta}_{21}$	Angular acceleration of link 2 for configuration 1
$\ddot{\theta}_{22}$	Angular acceleration of link 2 for configuration 2
$\varphi$	Direction angle of trajectory
$\varphi_{init}$	Initial direction angle of trajectory
$\varphi_{fin}$	Final direction angle of trajectory

<b>Acronym</b>	<b>Definiton</b>
----------------	------------------

DoF	Degree(s) of freedom
-----	----------------------

## ÖZET

# ÖNGÖRÜLEN BİR GÖREV SIRASINDA EN AZ ENERJİ SARFIYATI İÇİN İKİ SERBESTLİK DERECELİ BİR MANİPÜLATÖRÜN OPTİMUM KONUMUNUN TAYİNİ

**Mehmet Beşir KOPMAZ**

Bursa Teknik Üniversitesi

Fen Bilimleri Enstitüsü

Mekatronik Mühendisliği Bölümü

Yüksek Lisans Tezi

Yrd. Doç. Dr. İsmail BÜTÜN

Mart 2016, 47 Sayfa

Geçen birkaç on yılda robot manipülatörler verimli, hassas ve hızlı üretime olan devasa katkılarından ötürü seri üretimin vazgeçilemez unsuru haline gelmiştir. Öte yandan, enerjinin verimli kullanımının sınırlı enerji kaynakları ve bunların jeopolitik konumlarından ötürü birinci sanayi devriminden bugüne ana meselelerden biri olduğu iyi bilinen bir gerçektir. Enerjinin en büyük kullanıcılarından birinin imalat sanayi olduğu göz önüne alındığında üretim araçlarının ve bu bağlamda özellikle robotların zaman ve enerji bakımından optimal kullanımının önemi kolayca kavranabilir. Bu sebepten robotbilimde muhtelif kısıtlara maruz yörünge planlama başlığı altında ilgi çekici bir araştırma alanı ortaya çıkmıştır. Bu tez de verilen bir görev ve yörünge için enerji sarfiyatını en aza indirmeyle alakalıdır. Bu araştırma enerji sarfiyatını yeri belirlenmiş bir yörüngeye göre manipülatöre uygun bir yer bularak minimum yapmayı hedeflemesiyle önceki çalışmalardan farklılık arz etmektedir. Bu çalışmada yörüngelerin doğru parçaları şeklinde olduğu kabul edilmiştir. Ayrıca düzgün kinematik karakteristikleri olan sikloidal ve 3-4-5 polinom tipinde iki farklı hareket kanunu kullanılmaktadır. Sayısal sonuçlar manipülatör için enerji sarfiyatını minimum edecek tarzda her halükarda optimal bir konum bulmanın mümkün olduğunu ve 3-4-5 polinom hareket kanununun daha az enerji sarfiyatı sağladığını açıkça göstermektedir.

**Anahtar Sözcükler:** İki uzuvlu düzlemsel manipülatör, minimum enerji sarfiyatı, bir manipülatörün optimal konumu

## **ABSTRACT**

### **DETERMINATION OF THE OPTIMAL LOCATION OF A 2-DOF MANIPULATOR FOR MINIMAL ENERGY CONSUMPTION DURING A PREDEFINED TASK**

**Mehmet Beşir KOPMAZ**

Bursa Technical University

Graduate School of Natural and Applied Sciences

Department of Mechatronics Engineering

Master of Science Thesis

Asst. Prof. Dr. İsmail BÜTÜN

March 2016, 47 Pages

In the past several decades, robot manipulators have been indispensable part of serial production due to their huge contribution to the efficient, accurate and rapid manufacturing. On the other hand, it is a well-known fact that the efficient use of energy has been the main challenge from the first industrial revolution to date due to limited energy resources and their geo-political locations on the world. Considering that one of the largest consumers of energy is manufacturing industry, the importance of time- and energy-optimal usage of production machinery, specifically in this context can be well figured out. For this reason, in the field of robotics, an interesting research area has emerged under the headline of trajectory planning subject to different constraints among which time-optimal, energy-optimal or smooth (jerk- and impact-free) path tracking can be mentioned at first glance. This thesis is concerned with minimizing the energy consumption for a given task and trajectory. The present study differs from the previous work in that energy consumption is minimized by obtaining an appropriate location for the manipulator with respect to the trajectory fixed in the world coordinates. In this work, trajectories are assumed to be straight-lines. Besides, two different motion programs known with their smooth kinematic characteristics are tested, which are the cycloidal and the 3-4-5 polynomial motion programs. Numerical results obviously demonstrate that obtaining an optimal location for the manipulator regarding the use of minimal energy is possible, and the 3-4-5 polynomial motion program provides less energy consumption levels.

**Keywords:** 2-DoF planar manipulator, minimum energy consumption, optimal location of a manipulator



## 1. INTRODUCTION

In the past several decades, robots have become indispensable part of production lines due to their huge contribution to the efficient, accurate and rapid manufacturing. As a consequence of this, the trajectory planning subject to different constraints emerged as a new research area. Among them, time-optimal, energy-optimal or jerk-free trajectory planning can be mentioned at first glance. No doubt, energy resources and their efficient use have been the main challenge since the first industry revolution going back to the mid-19th century. Considering that one of large consumers of energy is manufacturing industry, the importance of time- and energy-optimal usage of robots can be well figured out. Although the subject has a long history extending to 1990's, it is still on the focus of researchers as the extensive literature on the subject indicates. However, to the author's knowledge, papers on energy-optimal path planning mostly deal with the problems in which starting, final and intermediate points of possible trajectory are given while the robot stands fixed. Some of the relevant papers develop and propose new methods that include almost all the parameters from the physical to control-related ones. These methods usually lead to fairly sophisticated optimization problems.

This thesis is concerned with the energy consumption of a 2-DoF planar manipulator. However, the present study differs from the previous work mainly in its conceptual novel approach. In this work, the position of production line is assumed to be stationary while the location of the manipulator can be changed in such a manner that the energy expenditure is reduced. In some sense, an inverse problem compared to the present literature is posed. Hence, the main purpose of this work is to find the suitable location of the manipulator for a predefined task so that the energy consumption be minimum. To make the proposed novel approach easily understandable, effects such as control parameters, damping, etc. are not considered. The numerical results obtained show that energy-optimal location is feasible for manipulators to be used in fixed production lines. The content of the work is limited with the solution of this problem for a 2-DoF planar manipulator.

## 2. LITERATURE SEARCH

As emphasized in the introduction, minimal energy based trajectory planning continues to be dealt with by researchers. As an indicator of this, here, some mentioning-worthy publications from the old to the recent ones will be referred to. In [1], Kopmaz *et al.* investigated the problem of finding an energy-optimal parabolic trajectory for a certain task which has some kinematic constraints in the start and end point of the trajectory. They used a finite number of trajectories which are defined with a parabolic equation on a pre-determined plane within the work space of a 6-DoF revolute manipulator, and showed that it is possible to find such a trajectory. Diken studied a similar problem in [2] using a sinusoidal path. Alshahrani *et al.* treated the problem of finding optimal trajectory function for minimum energy requirements of spherical robot, [3]. They assumed that the object to be manipulated follows a straight line in the work space. They choose three different displacement functions: simple harmonic, cycloidal and 3-4-5 polynomial. Compared to the energy consumption for bang-bang parabolic blend type displacement and cubic segment functions, the authors find out that cycloidal and 3-4-5 polynomial functions are tracked with more energy consumption while they provide a smooth running for the robot. If the energy consumption is the prime concern and the travel time is short, cubic segment trajectory is the best choice. Saramago *et al.* dealt with obtaining a trajectory subject to additional constraints for a PUMA-like robot such that a hybrid objective function consisting of weighted actuator powers and end effector grasping energy takes a minimum value, [4]. In [5], Verscheure *et al.* handled the problem of time-energy optimal path tracking. An objective function in which time does not appear explicitly is used. Through a nonlinear change of variables, the problem is transformed into a convex optimal control problem. De Santos *et al.* studied the energy required for six-legged robots which use alternating tripod gaits, and present a method aiming at reducing this energy need, [6]. Chen and Liao developed a hybrid strategy for the time- and energy-efficient trajectory planning for a 6-6 parallel platform, [7]. To this end, they proposed a cost function which consists of weighted functions of the consumed energy and time. In order to ensure the practical feasibility of the planned optimal trajectory, they took the physical constraints imposed by the parallel platform and actuator mechanism on the motion of the platform. The authors used the particle swarm optimization algorithm to obtain a crude estimate of the global optimal trajectory which is then supplied to the



conjugate gradient optimization method. They showed that this hybrid strategy outperforms the standalone particle swarm technique. In [8], Gasparetto *et al.* addressed the general problem of trajectory planning in Robotics. They give an overview of the most important methods proposed in the relevant literature especially to generate collision-free paths. In this work, it is expressed that the minimum time trajectory planning is very significant but this criterion certainly does not exhaust the possible applications or respond to all needs. In this context, the trajectory planning based on energy criteria has many interesting aspects. Such a planning produces smooth trajectories being easier to track and reduce the stresses to the actuators and the manipulator structure. In addition to that this approach allows energy saving which is very important for the cases in which energy source is limited like robotic applications for underwater exploration in military tasks. Gregory *et al.*, [9], investigated the issue of energy-optimal trajectory planning for robot manipulators with holonomic constraints. The authors employ a methodology to transform a variational problem with constraints to the one with no constraints. Hence, the problem take the form of an optimal control problem. They solved the problem on a simple SCARA robot which is a 2-DoF planar manipulator. They found solutions for different constraint types. In [10], Pellicciari *et al.* proposed a novel method implementable on both serial and parallel robots to minimize energy consumption which works in pick-and-place mode, and the trajectories of which are given by their starting, final and intermediate points. Mohammed *et al.* developed a different approach to minimize energy consumption. They carried out three scenarios with and without payload, and compared the results with those of commercial simulation software of the robot of interest. They developed a model searching the location of the energy-optimal path, [11]. Fung and Cheng dealt with a trajectory planning problem. They used the basic criterion of minimum absolute input energy (MAIE) to find the sought trajectory. The motion programs they used are parabolic blends, cycloidal, zero-jerk and polynomial ones. The polynomial was chosen of 12nd degree. The coefficients of this polynomial are obtained such that all the boundary conditions for the remaining three different trajectory profiles are satisfied. Then, energy consumptions for each profile are compared with each other. The authors use the real-coded genetic algorithm to find the energy optimal-polynomial for each case, [12]. Paes *et al.* determined the system parameters of an industrial ABB robot experimentally to find its energy efficient trajectories for a certain task. As a small case study, a typical pick-and-place maneuver

is both time- and energy-optimized. The authors subsequently compared these optimal trajectories to several straight-forward trajectories that are indicative for rotor operations in industry. To this end, they used the ACADO toolkit, an algorithm collection for automatic control and dynamic optimization. They proposed a non-invasive identification strategy for industrial robots, [13].

All the works mentioned above demonstrate that the energy consumption of robot manipulators will be a crucial topic in production activities when the issue of energy saving is considered to be of increasing significance. For this reason, in this thesis, energy optimization in manipulators are handled in a different way. For the case to be studied here, the trajectory is assumed to be a straight-line. However, for speed profile, two different functions are employed provided that they have same kinematic constraints. In contrast with the previous work, the energy-optimal location of the manipulator is sought under the assumption that the manipulation path is fixed in the world coordinates. Simulations and computational results show that there exist such optimal locations. For this purposes, a 2-DoF planar manipulator is considered. The choice of such a manipulator is only for simplicity because the first aim is to show how to work the methodology presented here. Firstly, an inverse kinematic analysis will be done. Meanwhile, the trial trajectories will be defined with its all kinematic parameters in such a manner that they are within the work space of the manipulator. Subsequently, for possible configurations of the robot, the energy consumption will be computed for different speed and acceleration profiles and constraints. Finally, the numerical results will be presented in graphics and commented.

### 3. INVERSE ANALYSIS

We consider the manipulator shown in Figure 3.1.

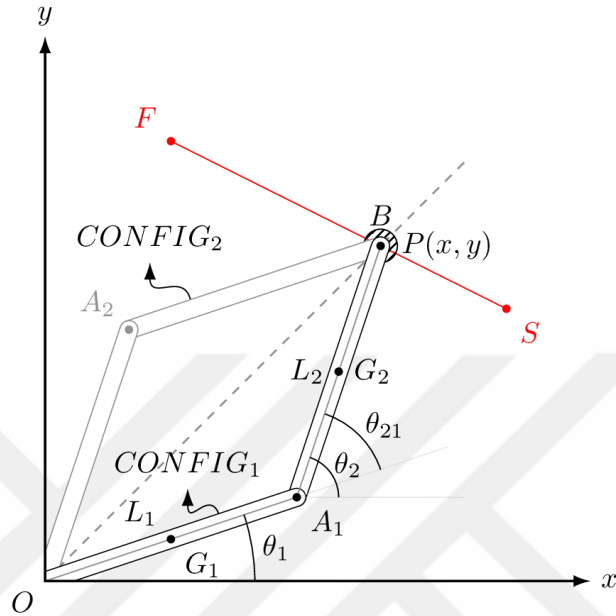


**Figure 3.1** Manipulator of interest

For a generic point  $P(x, y)$  in the  $xy$ -plane, there exist two different configurations of the manipulator, which are indicated with the abbreviations  $CONFIG_1$  and  $CONFIG_2$  in Figure 3.1 respectively. Furthermore, the straight-line  $SF$  is the trajectory to be followed by the end effector of the robot. Points  $S$  and  $F$  are the start and end points of the trajectory.  $L_1$  and  $L_2$  are the length of manipulator links. It is obvious that the work space is an annular region which is bounded by an outer circle with radius of  $L_1 + L_2$  and an inner circle with radius of  $|L_1 - L_2|$ . In practice, this region may be slightly different from the theoretical one due to physical constraints. In Figure 3.1,  $\theta_1$  and  $\theta_2$  are absolute rotation angles of two links in the world coordinates. However, the control angle of the second link is  $\theta_{21}$  in practical applications.

### 3.1. Position Analysis

From Figure 3.1, the following equations are easily written:

$$L_1 \cos \theta_1 + L_2 \cos \theta_2 = x \quad (3.1a)$$

$$L_1 \sin \theta_1 + L_2 \sin \theta_2 = y \quad (3.1b)$$

First, angle  $\theta_1$  is to be formulated. Therefore, the terms including  $\theta_2$  are left alone on the right side of the equations.

$$L_2 \cos \theta_2 = x - L_1 \cos \theta_1 \quad (3.2a)$$

$$L_2 \sin \theta_2 = y - L_1 \sin \theta_1 \quad (3.2b)$$

Taking square of both sides and adding side by side, the equation below is obtained:

$$L_2^2 = x^2 + y^2 + L_1^2 - 2xL_1 \cos \theta_1 - 2yL_1 \sin \theta_1 \quad (3.3a)$$

Rearranging 3.3a it we obtain:

$$-2xL_1 \cos \theta_1 - 2yL_1 \sin \theta_1 + x^2 + y^2 + L_1^2 - L_2^2 = 0 \quad (3.3b)$$

Let us define:

$$a := -2xL_1 \quad (3.4a)$$

$$b := -2yL_1 \quad (3.4b)$$

$$c := x^2 + y^2 + L_1^2 - L_2^2 \quad (3.4c)$$

$$\lambda := \tan \frac{\theta_1}{2} \quad (3.4d)$$

As is well-known from trigonometry, the following relationships exist:

$$\cos \theta_1 = \frac{1 - \lambda^2}{1 + \lambda^2} \quad (3.5a)$$

$$\sin \theta_1 = \frac{2\lambda}{1 + \lambda^2} \quad (3.5b)$$

Using (3.4) and (3.5) in (3.3b) one finds:

$$(1 - \lambda^2)a + 2b\lambda + (1 + \lambda^2)c = 0 \quad (3.6a)$$

or

$$(c - a)\lambda^2 + 2b\lambda + (c + a) = 0 \quad (3.6b)$$

Now, similar to the first three of (3.4), we define

$$A := c - a \quad (3.7a)$$

$$B := b \quad (3.7b)$$

$$C := c + a \quad (3.7c)$$

Substituting (3.7) in (3.6) gives the equation

$$A\lambda^2 + 2B\lambda + C = 0 \quad (3.8)$$

the roots of which are

$$\lambda_1 = \frac{-B - \sqrt{B^2 - AC}}{A} \quad (3.9a)$$

$$\lambda_2 = \frac{-B + \sqrt{B^2 - AC}}{A} \quad (3.9b)$$

respectively. Hence we have two distinct values for  $\theta_1$ :

$$\theta_{1,1} = 2 \tan^{-1} \lambda_1 \quad (3.10a)$$

$$\theta_{1,2} = 2 \tan^{-1} \lambda_2 \quad (3.10b)$$

where the second subscript refers to these distinct values of  $\theta_1$ , which implies that there exist two possible configurations of the robot to reach point  $P$ . From equation (3.2), the variants of  $\theta_2$  can be found as follows:

$$\sin \theta_{2,i} = \frac{y - L_1 \sin \theta_{1,i}}{L_2}, \quad i = 1,2 \quad (3.11a)$$

$$\cos \theta_{2,i} = \frac{x - L_1 \cos \theta_{1,i}}{L_2}, \quad i = 1,2 \quad (3.11b)$$

Which of these alternatives are used depends on the assembly of robot in the beginning.

### 3.2. Velocity Analysis

Derivation of equations (3.1) with respect to time will give the angular velocities of the links in the world coordinates:

$$-L_1 \sin \theta_1 \dot{\theta}_1 - L_2 \sin \theta_2 \dot{\theta}_2 = \dot{x} \quad (3.12a)$$

$$L_1 \cos \theta_1 \dot{\theta}_1 + L_2 \cos \theta_2 \dot{\theta}_2 = \dot{y} \quad (3.12b)$$

Let us rewrite equation (3.12) in the matrix form:

$$\begin{bmatrix} -L_1 \sin \theta_1 & -L_2 \sin \theta_2 \\ L_1 \cos \theta_1 & L_2 \cos \theta_2 \end{bmatrix} \begin{bmatrix} \dot{\theta}_1 \\ \dot{\theta}_2 \end{bmatrix} = \begin{bmatrix} \dot{x} \\ \dot{y} \end{bmatrix} \quad (3.13)$$

Using Cramer Method the following expressions are obtained:

$$\dot{\theta}_1 = \frac{\cos \theta_2}{\sin(\theta_2 - \theta_1)} \frac{\dot{x}}{L_1} + \frac{\sin \theta_2}{\sin(\theta_2 - \theta_1)} \frac{\dot{y}}{L_1} \quad (3.14a)$$

$$\dot{\theta}_2 = \frac{\cos \theta_1}{\sin(\theta_2 - \theta_1)} \frac{\dot{x}}{L_2} + \frac{\sin \theta_1}{\sin(\theta_2 - \theta_1)} \frac{\dot{y}}{L_2} \quad (3.14b)$$

where  $\dot{x}$  and  $\dot{y}$  are the components of the end point in  $x$ - and  $y$ -direction.

### 3.3. Acceleration Analysis

Taking time derivatives of equations (3.12) gives the equations needed to find angular accelerations:

$$-L_1 \cos \theta_1 \dot{\theta}_1^2 - L_1 \sin \theta_1 \ddot{\theta}_1 - L_2 \cos \theta_2 \dot{\theta}_2^2 - L_2 \sin \theta_2 \ddot{\theta}_2 = \ddot{x} \quad (3.15a)$$

$$-L_1 \sin \theta_1 \dot{\theta}_1^2 + L_1 \cos \theta_1 \ddot{\theta}_1 - L_2 \sin \theta_2 \dot{\theta}_2^2 + L_2 \cos \theta_2 \ddot{\theta}_2 = \ddot{y} \quad (3.15b)$$

Let us put equation (3.15) into the matrix form:

$$\begin{bmatrix} -L_1 \sin \theta_1 & -L_2 \sin \theta_2 \\ L_1 \cos \theta_1 & L_2 \cos \theta_2 \end{bmatrix} \begin{bmatrix} \ddot{\theta}_1 \\ \ddot{\theta}_2 \end{bmatrix} = \begin{bmatrix} \ddot{x} + L_1 \cos \theta_1 \dot{\theta}_1^2 + L_2 \cos \theta_2 \dot{\theta}_2^2 \\ \ddot{y} + L_1 \sin \theta_1 \dot{\theta}_1^2 + L_2 \sin \theta_2 \dot{\theta}_2^2 \end{bmatrix} \quad (3.16)$$

For simplicity, let the followings be defined:

$$\gamma_1 := \ddot{x} + L_1 \cos \theta_1 \dot{\theta}_1^2 + L_2 \cos \theta_2 \dot{\theta}_2^2 \quad (3.17a)$$

$$\gamma_2 := \ddot{y} + L_1 \sin \theta_1 \dot{\theta}_1^2 + L_2 \sin \theta_2 \dot{\theta}_2^2 \quad (3.17b)$$

Then we obtain the angular accelerations as follows:

$$\ddot{\theta}_1 = \frac{\cos \theta_2}{\sin(\theta_2 - \theta_1)} \frac{\gamma_1}{L_1} + \frac{\sin \theta_2}{\sin(\theta_2 - \theta_1)} \frac{\gamma_2}{L_1} \quad (3.17a)$$

$$\ddot{\theta}_2 = \frac{\cos \theta_1}{\sin(\theta_2 - \theta_1)} \frac{\gamma_1}{L_2} + \frac{\sin \theta_1}{\sin(\theta_2 - \theta_1)} \frac{\gamma_2}{L_2} \quad (3.17b)$$

With these formulas obtained, the inverse kinematic analysis of the manipulator has been completed.

#### 4. DEFINITION OF TASK AND SEARCHING OPTIMAL TRAJECTORY

In this work, it is assumed that the task to be executed by the considered planar manipulator is to carry a body of mass  $m$  in the end effector from a starting point  $S$  to a final point  $F$  along a straight line of length  $L$  in  $T$  seconds. However, different motion programs, i.e. different velocity and acceleration profiles, can be tested. In all cases, kinematic constraints at point  $S$  and point  $F$  will be held same. For a trajectory of certain length  $L$ , once a starting point within the workspace of manipulator, in our study on the  $x$ -axis specifically, is chosen the limit values of the direction angle of trajectory  $\varphi$  are to be obtained. Let the initial value of this angle be  $\varphi_{init}$ . It is found such that the final point of the first trial trajectory stay on the outer boundary of workspace, which is a circle of radius  $L_1 + L_2$ . Similarly, the final value of  $\varphi$ , i.e.  $\varphi_{fin}$ , is obtained considering that the final point of trajectory must stay either on the  $x$ -axis or, in the most critical case, on the inner boundary of the workspace, which is a circle of radius  $|L_1 - L_2|$ . Since the workspace is an annular region being symmetric with respect to the  $x$ -axis, it is sufficient to confine all the search activity only in the upper semi-plane. Again, for a given length of trajectory, observing the constraint that the final point of trajectory must be on the outer boundary of workspace, the final or minimum value that  $x_S$  can take is calculated. Note that the coordinates of all starting points are in the form of  $(x_S, 0)$ , in other saying, the ordinates of those points will be taken zero without loss of generality. According to what is just mentioned, given the length of trajectory  $L$  and the abscissa of starting point  $x_S$ ,  $x_{S_{fin}}$  must be determined first. Recall that the initial value of  $x_S$  is same for all trajectory lengths and equal to  $L_1 + L_2$ . Then, for a chosen  $x_S$ , the limit values of direction angle  $\varphi$ , i.e.  $\varphi_{init}$  and  $\varphi_{fin}$ , have to be obtained. Once the initial trial trajectory is defined, for each  $\varphi$  value which is increased with a certain increment, say  $1^\circ$ , the energy consumption can be computed for each trajectory having the same starting point. Afterwards, among these trial trajectories, the one on which minimal energy is spent is selected as the optimal one. Assuming that this optimal trajectory is fixed in the space, the root point of the manipulator is determined. It is worth noting for the completeness of the study that any point on any radius within the annular region can be taken as starting point  $S$  during the execution of task.

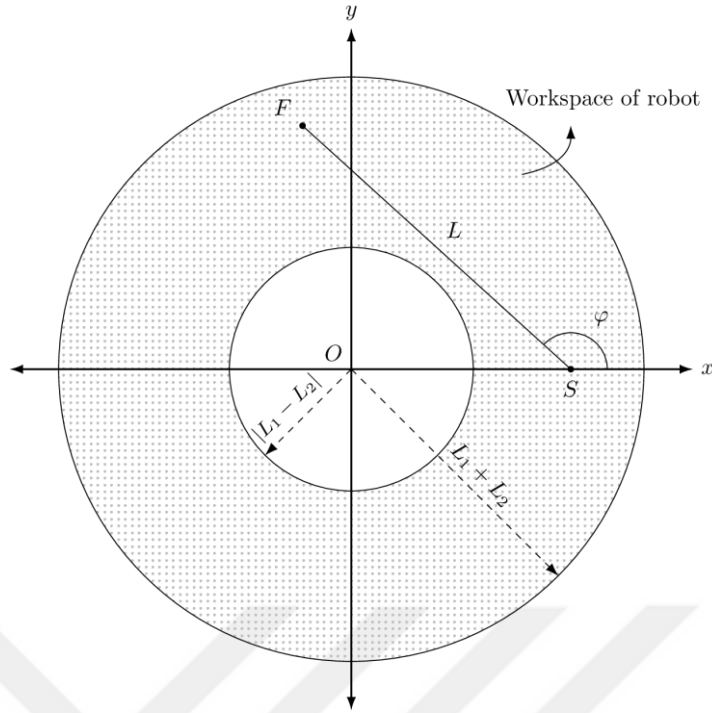


**Figure 4.1** Geometric definition of trajectory

Before giving the details of the strategy of searching trial trajectories, it will be explained how to describe a generic trajectory in the following. As is well-known, the equation of a straight line in the  $xy$ -plane as follows:

$$y = mx + n \quad (4.1)$$

where

$$m := \tan \varphi = \frac{y_F - y_S}{x_F - x_S} \quad (4.2a)$$

$$n := y_S x_F - y_F x_S \quad (4.2b)$$

with  $(x_S, y_S)$  and  $(x_F, y_F)$  being the coordinates of points  $S$  and  $F$  respectively.

Defining a unit vector  $\mathbf{u}$  will be useful for future calculations:

$$\mathbf{u} := \cos \varphi \mathbf{i} + \sin \varphi \mathbf{j} \quad (4.3)$$

The position vector of any point on the trajectory will be as below:

$$\mathbf{r} := \mathbf{r}_S + s \mathbf{u}, \quad 0 \leq s \leq L \quad (4.4)$$



where  $\mathbf{r}_S$  is the position vector of starting point  $S$ , i.e.

$$\mathbf{r}_S := x_S \mathbf{i} + y_S \mathbf{j} \quad (4.5)$$

and  $s$  is the distance travelled by the end effector from starting point  $S$  at any time  $t$ . It is obvious that  $s = s(t)$  and the form of relation between  $s$  and  $t$  depends on the motion program used, see Figure 4.1.

Now, possible trial trajectories will be discussed. The longest possible trajectory is shown in Figure 4.2. Accordingly, its length is as follows:

$$L_{max} = 2\sqrt{(L_1 + L_2)^2 - (L_1 - L_2)^2} = 2\sqrt{4L_1L_2} = 4\sqrt{L_1L_2} \quad (4.6)$$

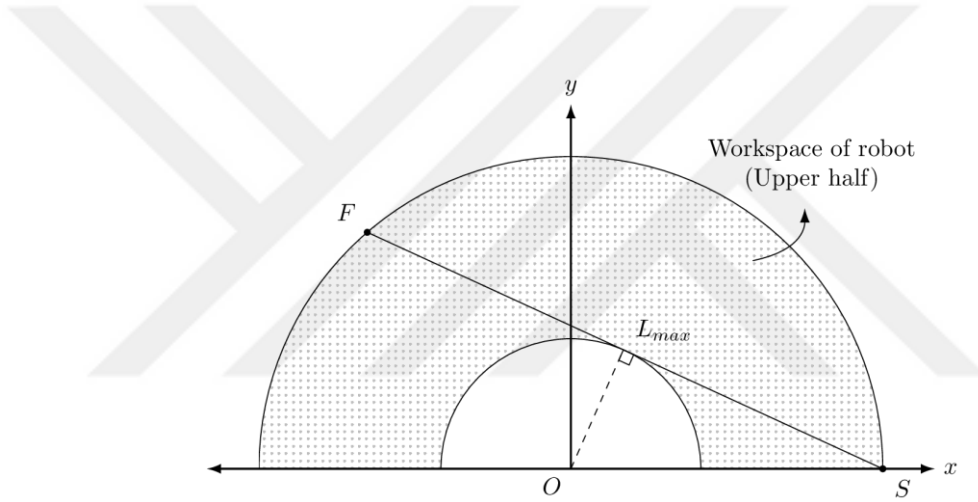


**Figure 4.2** The longest possible trajectory

The length of trial trajectories cannot be greater than this value. Obviously, there exists only one trajectory whose length is  $L_{max}$ . Now, three cases for the interval of  $x_S$  values are distinguished depending upon the length of trajectory:

**CASE 1:**  $L = L_{max}$

$$x_{S_{init}} = x_{S_{fin}} = L_1 + L_2 \quad (4.7)$$

**CASE 2:**  $L_{max}/2 < L < L_{max}$

$$x_{S_{init}} = L_1 + L_2 \quad (4.8a)$$

$$x_{S_{fin}} = \sqrt{(L_1 + L_2)^2 + L^2 - 2(L_1 + L_2)L \cos \left[ \sin^{-1} \left( \frac{L_1 - L_2}{L_1 + L_2} \right) \right]} \quad (4.8b)$$

**CASE 3:**  $L \leq L_{max}/2$

$$x_{S_{init}} = L_1 + L_2 \quad (4.9a)$$

$$x_{S_{fin}} = |L_1 - L_2| \quad (4.9b)$$

Similar to the above case study, for a certain length of trajectory and given  $x_S$  value, the main and subcases are distinguished to determine the interval of  $\varphi$  values:

**CASE 1:**  $L = L_{max}$

$$\varphi_{init} = \varphi_{fin} = \pi - \sin^{-1} \left( \frac{L_1 - L_2}{L_1 + L_2} \right) \quad (4.10)$$

**CASE 2:**  $L_{max}/2 \leq L < L_{max}$

$$\varphi_{init} = \pi - \cos^{-1} \left[ \frac{L^2 + x_S^2 - (L_1 + L_2)^2}{2Lx_S} \right] \quad (4.11a)$$

$$\varphi_{fin} = \pi - \sin^{-1} \left( \frac{L_1 - L_2}{x_S} \right) \quad (4.11b)$$

**CASE 3:**  $2L_2 < L < L_{max}/2$

$$\varphi_{init} = \pi - \cos^{-1} \left[ \frac{L^2 + x_S^2 - (L_1 + L_2)^2}{2Lx_S} \right] \quad (4.12a)$$

$$\alpha := \cos^{-1} \left( \frac{L_1 - L_2}{x_S} \right) \quad (4.12b)$$

$$\varphi_{fin} = \begin{cases} \pi - \left( \frac{\pi}{2} - \alpha \right), & x_S \sin \alpha \leq L \end{cases} \quad (4.12c)$$

$$\varphi_{fin} = \begin{cases} \pi - \cos^{-1} \left[ \frac{L^2 + x_S^2 - (L_1 - L_2)^2}{2Lx_S} \right], & x_S \sin \alpha > L \end{cases} \quad (4.12d)$$

**CASE 4:  $L \leq 2L_2$** **Subcase 4.1:  $L_1 + L_2 - x_S \geq L$** 

$$\varphi_{init} = 0 \quad (4.13a)$$

$$\varphi_{fin} = \begin{cases} \pi, & x_S - (L_1 - L_2) \geq L \quad (4.13b) \\ \pi - \cos^{-1} \left[ \frac{L^2 + x_S^2 - (L_1 - L_2)^2}{2Lx_S} \right], & x_S - (L_1 - L_2) < L \quad (4.13c) \end{cases}$$

**Subcase 4.2:  $L_1 + L_2 - x_S < L$** 

$$\varphi_{init} = \pi - \cos^{-1} \left[ \frac{L^2 + x_S^2 - (L_1 + L_2)^2}{2Lx_S} \right] \quad (4.13d)$$

$$\varphi_{fin} = \begin{cases} \pi, & x_S - (L_1 - L_2) \geq L \quad (4.13e) \\ \pi - \cos^{-1} \left[ \frac{L^2 + x_S^2 - (L_1 - L_2)^2}{2Lx_S} \right], & x_S - (L_1 - L_2) < L \quad (4.13f) \end{cases}$$

The computational procedure will work in the following way:

1. Choose a length of trajectory  $L$  noting it must be smaller than or equal to  $L_{max}$ .
2. From the formulas (4.7) to (4.9), use the appropriate one for the chosen length, and find  $x_{S_{fin}}$ .
3. Determine that the interval of  $x_S$  will be divided to how many subinterval. The step size  $\Delta x$  between successive starting points can be found dividing the interval  $|x_{S_{fin}} - x_{S_{init}}|$  by  $nx_S$ . The number of starting points to be used during computation is then  $(|x_{S_{fin}} - x_{S_{init}}|/\Delta x) + 1$ .
4. For a starting point chosen, use the appropriate one between formulas (4.10) to (4.13) to obtain then interval of direction angle  $\varphi$  for the starting point chosen and the given length.
5. Find the number of straight-lines in the bunch of trial trajectories dividing the interval  $|\varphi_{fin} - \varphi_{init}|$  by  $\Delta\varphi$ . Hence, the number of these points equals to  $(|\varphi_{fin} - \varphi_{init}|/\Delta\varphi) + 1$ .
6. For each of trial trajectories, compute the energy consumption and store them.
7. Repeat the procedure for other starting points.
8. Obtain the trajectory for which minimum energy is consumed.

9. Plot all relevant graphics, e.g. displacement, angular velocities and accelerations, actuator torques, energy consumption curves for the energy-optimal trajectory.

Usually in the practice, repositioning of a production or assembly line is quite difficult. If a robot arm is to be introduced into such a production line, then the only alternative is to find such an appropriate location for the robot that the energy consumption during that pre-defined operation be minimal. In this case, especially for the trajectory discussed here, a new coordinate system is defined as shown in Figure 4.3 to fix the location of the robot with respect to the trajectory, or in some sense, production line. In this new coordinate system, the position of the root of robot arm can be obtained just using the starting point  $x_S$  and the orientation angle  $\varphi$  of the energy-optimal trajectory. Consequently, these coordinates are obtained as follows:

$$X = -x_S \cos \varphi \quad (4.14a)$$

$$Y = x_S \sin \varphi \quad (4.14b)$$

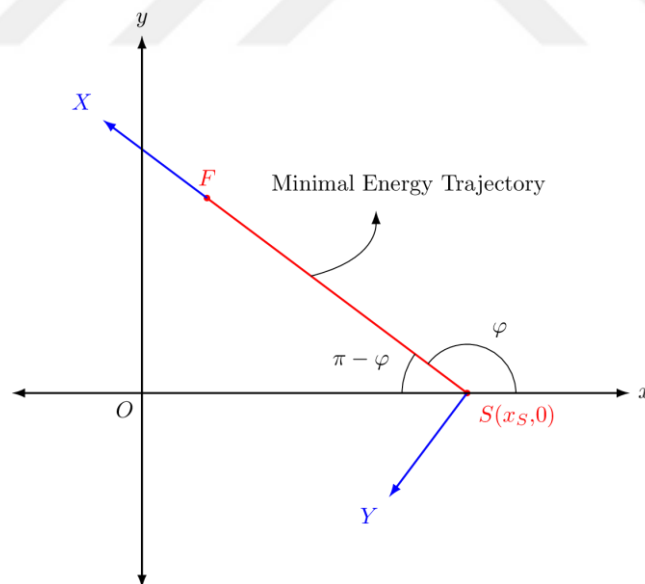


**Figure 4.3** New coordinate system with respect to minimal energy trajectory

## 5. KINEMATIC CONSTRAINTS, VELOCITY AND ACCELERATION FUNCTIONS

The kinematic constraints are given below:

$$\text{at } t = 0, \quad s(0) = 0, \quad \dot{s}(0) = 0, \quad \ddot{s}(0) = 0 \quad (5.1a)$$

$$\text{at } t = T, \quad s(T) = L, \quad \dot{s}(T) = 0, \quad \ddot{s}(T) = 0 \quad (5.1b)$$

where  $s$ ,  $\dot{s}$  and  $\ddot{s}$  show the displacement on the trajectory, its first time derivative and its second time derivation respectively. Kinematic constraints are given by equations (5.1) imply that the motion at the beginning and at the end must be impact- and jerk-free. In this work, two different displacement functions will be used. One of them is a cycloidal displacement function while the other is a 3-4-5 polynomial. Consequently, the displacement, velocity and acceleration functions are as follows:

### Cycloidal Motion:

$$s(t) = L \left( \frac{t}{T} - \frac{1}{2\pi} \sin \frac{2\pi t}{T} \right) \quad (5.2a)$$

$$\dot{s}(t) = \frac{L}{T} \left( 1 - \cos \frac{2\pi t}{T} \right) \quad (5.2b)$$

$$\ddot{s}(t) = \frac{2\pi L}{T^2} \sin \frac{2\pi t}{T} \quad (5.2c)$$

### 3-4-5 Polynomial Motion:

$$s(t) = L \left[ 6 \left( \frac{t}{T} \right)^5 - 15 \left( \frac{t}{T} \right)^4 + 10 \left( \frac{t}{T} \right)^3 \right] \quad (5.3a)$$

$$\dot{s}(t) = \frac{L}{T} \left[ 30 \left( \frac{t}{T} \right)^4 - 60 \left( \frac{t}{T} \right)^3 + 30 \left( \frac{t}{T} \right)^2 \right] \quad (5.3b)$$

$$\ddot{s}(t) = \frac{L}{T^2} \left[ 120 \left( \frac{t}{T} \right)^3 - 180 \left( \frac{t}{T} \right)^2 + 60 \left( \frac{t}{T} \right)^1 \right] \quad (5.3c)$$

## 6. EQUATIONS OF MOTION

This section is devoted to deriving equations of motion by using Lagrangian approach. As is well-known, the first step of this approach is to obtain kinetic and potential energy terms of the system. Hence the linear velocities of certain system points like center of gravities and joints. These points are  $G_1$ ,  $A_1$ ,  $G_2$  and  $B$  (see Figure 3.1). Velocity of point  $G_1$ :

$$\begin{aligned}\mathbf{v}_{G_1} &= \dot{\theta}_1 \mathbf{k} \times (r_{G_1} \cos \theta_1 \mathbf{i} + r_{G_1} \sin \theta_1 \mathbf{j}) \\ &= -r_{G_1} \sin \theta_1 \dot{\theta}_1 \mathbf{i} + r_{G_1} \cos \theta_1 \dot{\theta}_1 \mathbf{j}\end{aligned}\quad (6.1)$$

where  $r_{G_1} = \overline{OG_1}$  and  $\dot{\theta}_1 \mathbf{k}$  is the angular velocity of link 1. From (6.1) one obtains:

$$\mathbf{v}_{G_1}^2 = \mathbf{v}_{G_1} \cdot \mathbf{v}_{G_1} = r_{G_1}^2 \dot{\theta}_1^2 \quad (6.2)$$

Velocity of point  $A$ :

$$\begin{aligned}\mathbf{v}_A &= \dot{\theta}_1 \mathbf{k} \times (L_1 \cos \theta_1 \mathbf{i} + L_1 \sin \theta_1 \mathbf{j}) \\ &= -L_1 \sin \theta_1 \dot{\theta}_1 \mathbf{i} + L_1 \cos \theta_1 \dot{\theta}_1 \mathbf{j}\end{aligned}\quad (6.3)$$

From (6.3) we find:

$$\mathbf{v}_A^2 = \mathbf{v}_A \cdot \mathbf{v}_A = L_1^2 \dot{\theta}_1^2 \quad (6.4)$$

Velocity of point  $G_2$ :

$$\mathbf{v}_{G_2} = \mathbf{v}_A + \mathbf{v}_{G_2/A} \quad (6.5)$$

$$\begin{aligned}\mathbf{v}_{G_2/A} &= \dot{\theta}_2 \mathbf{k} \times (r_{G_2} \cos \theta_2 \mathbf{i} + r_{G_2} \sin \theta_2 \mathbf{j}) \\ &= -r_{G_2} \sin \theta_2 \dot{\theta}_2 \mathbf{i} + r_{G_2} \cos \theta_2 \dot{\theta}_2 \mathbf{j}\end{aligned}\quad (6.6)$$

$$\begin{aligned}\mathbf{v}_{G_2} &= -(L_1 \sin \theta_1 \dot{\theta}_1 + r_{G_2} \sin \theta_2 \dot{\theta}_2) \mathbf{i} \\ &\quad + (L_1 \cos \theta_1 \dot{\theta}_1 + r_{G_2} \cos \theta_2 \dot{\theta}_2) \mathbf{j}\end{aligned}\quad (6.7)$$

Similarly, from (6.7) one finds:

$$\mathbf{v}_{G_2}^2 = \mathbf{v}_{G_2} \cdot \mathbf{v}_{G_2} = L_1^2 \dot{\theta}_1^2 + r_{G_2}^2 \dot{\theta}_2^2 + 2L_1 r_{G_2} \cos(\theta_2 - \theta_1) \dot{\theta}_1 \dot{\theta}_2 \quad (6.8)$$

Velocity of point  $B$ :

$$\mathbf{v}_B = \mathbf{v}_A + \mathbf{v}_{B/A} \quad (6.9)$$

$$\begin{aligned} \mathbf{v}_{B/A} &= \dot{\theta}_2 \mathbf{k} \times (L_2 \cos \theta_2 \mathbf{i} + L_2 \sin \theta_2 \mathbf{j}) \\ &= -L_2 \sin \theta_2 \dot{\theta}_2 \mathbf{i} + L_2 \cos \theta_2 \dot{\theta}_2 \mathbf{j} \end{aligned} \quad (6.10)$$

$$\begin{aligned} \mathbf{v}_B &= -(L_1 \sin \theta_1 \dot{\theta}_1 + L_2 \sin \theta_2 \dot{\theta}_2) \mathbf{i} \\ &\quad + (L_1 \cos \theta_1 \dot{\theta}_1 + L_2 \cos \theta_2 \dot{\theta}_2) \mathbf{j} \end{aligned} \quad (6.11)$$

Taking square of  $|\mathbf{v}_B|$  yields:

$$\mathbf{v}_B^2 = \mathbf{v}_B \cdot \mathbf{v}_B = L_1^2 \dot{\theta}_1^2 + L_2^2 \dot{\theta}_2^2 + 2L_1 L_2 \cos(\theta_2 - \theta_1) \dot{\theta}_1 \dot{\theta}_2 \quad (6.12)$$

Kinetic energy of link 1:

$$\begin{aligned} T_1 &= \frac{1}{2} I_{G_1} \dot{\theta}_1^2 + \frac{1}{2} m_1 v_{G_1}^2 \\ &= \frac{1}{2} I_{G_1} \dot{\theta}_1^2 + \frac{1}{2} m_1 r_{G_1}^2 \dot{\theta}_1^2 \\ &= \frac{1}{2} (I_{G_1} + m_1 r_{G_1}^2) \dot{\theta}_1^2 \end{aligned} \quad (6.13)$$

According to the parallel-axes theorem we can define:

$$I_{1,O} := I_{G_1} + m_1 r_{G_1}^2 \quad (6.14)$$

where  $I_{1,O}$  is the mass moment of inertia of link 1 about the axis through the joint at  $O$ .

Kinetic energy of link 2:

$$\begin{aligned} T_2 &= \frac{1}{2} I_{G_2} \dot{\theta}_2^2 + \frac{1}{2} m_2 v_{G_2}^2 \\ &= \frac{1}{2} I_{G_2} \dot{\theta}_2^2 + \frac{1}{2} m_2 [L_1^2 \dot{\theta}_1^2 + r_{G_2}^2 \dot{\theta}_2^2] + 2L_1 r_{G_2} \cos(\theta_2 - \theta_1) \dot{\theta}_1 \dot{\theta}_2 \end{aligned} \quad (6.15)$$

Here we also define:

$$I_{2,A} := I_{G_2} + m_2 r_{G_2}^2 \quad (6.16)$$

where  $I_{2,A}$  is the mass moment of inertia of link 2 about the axis through the joint at  $A$ .

Consequently, equation (6.15) can be written as follows:

$$I_2 = \frac{1}{2}I_{2,A}\dot{\theta}_2^2 + \frac{1}{2}m_2L_1^2\dot{\theta}_1^2 + m_2L_1r_{G_2}\cos(\theta_2 - \theta_1)\dot{\theta}_1\dot{\theta}_2 \quad (6.17)$$

Kinetic energy of the object of mass  $m$  carried with end effector:

$$T_m = \frac{1}{2}mv_B^2 = \frac{1}{2}m[L_1^2\dot{\theta}_1^2 + L_2^2\dot{\theta}_2^2] + mL_1L_2\cos(\theta_2 - \theta_1)\dot{\theta}_1\dot{\theta}_2 \quad (6.18)$$

Virtual works of actuator torques:

Actuator 1:

$$\delta W_1 = \mathbf{M}_1 \cdot \delta \boldsymbol{\theta}_1 = M_1 \mathbf{k} \cdot \delta \theta_1 \mathbf{k} = M_1 \delta \theta_1 \quad (6.19)$$

Actuator 2:

$$\begin{aligned} \delta W_2 &= \mathbf{M}_2 \cdot (\delta \boldsymbol{\theta}_2 - \delta \boldsymbol{\theta}_1) \\ &= M_2 \mathbf{k} \cdot (\delta \theta_2 \mathbf{k} - \delta \theta_1 \mathbf{k}) \\ &= M_2 \delta \theta_2 - M_2 \delta \theta_1 \end{aligned} \quad (6.20)$$

Total virtual work:

$$\begin{aligned} \delta W &= \delta W_1 + \delta W_2 \\ &= (M_1 - M_2) \delta \theta_1 + M_2 \delta \theta_2 \end{aligned} \quad (6.21)$$

Total kinetic energy:

$$\begin{aligned} T &= T_1 + T_2 + T_m \\ &= \frac{1}{2}I_{1,O}\dot{\theta}_1^2 + \frac{1}{2}I_{2,A}\dot{\theta}_2^2 + \frac{1}{2}m_2L_1^2\dot{\theta}_1^2 \\ &\quad + m_2L_1r_{G_2}\cos(\theta_2 - \theta_1)\dot{\theta}_1\dot{\theta}_2 \\ &\quad + \frac{1}{2}m[L_1^2\dot{\theta}_1^2 + L_2^2\dot{\theta}_2^2] + mL_1L_2\cos(\theta_2 - \theta_1)\dot{\theta}_1\dot{\theta}_2 \end{aligned} \quad (6.22)$$

or rearranging we find:

$$\begin{aligned} T &= \frac{1}{2}(I_{1,O} + m_2L_1^2 + mL_1^2)\dot{\theta}_1^2 + \frac{1}{2}(I_{2,A} + mL_2^2)\dot{\theta}_2^2 \\ &\quad + (m_2L_1r_{G_2} + mL_1L_2)\cos(\theta_2 - \theta_1)\dot{\theta}_1\dot{\theta}_2 \end{aligned} \quad (6.23)$$



### Equation of Motion of Link 1:

According to the Lagrangian mechanics, the equation of motion is given by the following formula:

$$\frac{d}{dt} \left( \frac{\partial T}{\partial \dot{\theta}_1} \right) - \frac{\partial T}{\partial \theta_1} = Q_1 \quad (6.24)$$

where

$$Q_1 := M_1 - M_2 \quad (6.25)$$

Let us calculate the terms on the left side of equation (6.24):

$$\frac{\partial T}{\partial \dot{\theta}_1} = [I_{1,0} + (m_2 + m)L_1^2] \dot{\theta}_1 + (m_2 L_1 r_{G_2} + m L_1 L_2) \cos(\theta_2 - \theta_1) \dot{\theta}_2 \quad (6.26)$$

Therefore,

$$\begin{aligned} \frac{d}{dt} \left( \frac{\partial T}{\partial \dot{\theta}_1} \right) &= [I_{1,0} + (m_2 + m)L_1^2] \ddot{\theta}_1 \\ &\quad - (m_2 L_1 r_{G_2} + m L_1 L_2) \sin(\theta_2 - \theta_1) \dot{\theta}_2^2 \\ &\quad + (m_2 L_1 r_{G_2} + m L_1 L_2) \cos(\theta_2 - \theta_1) \ddot{\theta}_2 \\ &\quad + (m_2 L_1 r_{G_2} + m L_1 L_2) \sin(\theta_2 - \theta_1) \dot{\theta}_1 \dot{\theta}_2 \end{aligned} \quad (6.27)$$

and

$$\begin{aligned} \frac{\partial T}{\partial \theta_1} &= -(m_2 L_1 r_{G_2} + m L_1 L_2) \sin(\theta_2 - \theta_1) (-1) \dot{\theta}_1 \dot{\theta}_2 \\ &= (m_2 L_1 r_{G_2} + m L_1 L_2) \sin(\theta_2 - \theta_1) \dot{\theta}_1 \dot{\theta}_2 \end{aligned} \quad (6.28)$$

Substituting equations (6.25), (6.27) and (6.28) in equation (6.24) yields

$$\begin{aligned} M_1 - M_2 &= [I_{1,0} + (m_2 + m)L_1^2] \ddot{\theta}_1 \\ &\quad + (m_2 L_1 r_{G_2} + m L_1 L_2) \cos(\theta_2 - \theta_1) \ddot{\theta}_2 \\ &\quad - (m_2 L_1 r_{G_2} + m L_1 L_2) \sin(\theta_2 - \theta_1) \dot{\theta}_2^2 \end{aligned} \quad (6.29)$$

### Equation of Motion of Link 2:

The Lagrangian form of the equation of motion for link 2 is as follows:

$$\frac{d}{dt} \left( \frac{\partial T}{\partial \dot{\theta}_2} \right) - \frac{\partial T}{\partial \theta_2} = Q_2 \quad (6.30)$$

where

$$Q_2 := M_2 \quad (6.31)$$

Let us calculate the terms on the left side of equation (6.30):

$$\frac{\partial T}{\partial \dot{\theta}_2} = (I_{2,A} + mL_2^2) \dot{\theta}_2 + (m_2 L_1 r_{G_2} + mL_1 L_2) \cos(\theta_2 - \theta_1) \dot{\theta}_1 \quad (6.32)$$

Therefore

$$\begin{aligned} \frac{d}{dt} \left( \frac{\partial T}{\partial \dot{\theta}_2} \right) &= (I_{2,A} + mL_2^2) \ddot{\theta}_2 \\ &\quad - (m_2 L_1 r_{G_2} + mL_1 L_2) \sin(\theta_2 - \theta_1) (\dot{\theta}_2 - \dot{\theta}_1) \dot{\theta}_1 \\ &\quad + (m_2 L_1 r_{G_2} + mL_1 L_2) \cos(\theta_2 - \theta_1) \ddot{\theta}_1 \\ &= (I_{2,A} + mL_2^2) \ddot{\theta}_2 + (m_2 L_1 r_{G_2} + mL_1 L_2) \sin(\theta_2 - \theta_1) \dot{\theta}_1^2 \\ &\quad + (m_2 L_1 r_{G_2} + mL_1 L_2) \cos(\theta_2 - \theta_1) \ddot{\theta}_1 \\ &\quad - (m_2 L_1 r_{G_2} + mL_1 L_2) \sin(\theta_2 - \theta_1) \dot{\theta}_1 \ddot{\theta}_2 \end{aligned} \quad (6.33)$$

and

$$\frac{\partial T}{\partial \theta_2} = -(m_2 L_1 r_{G_2} + mL_1 L_2) \sin(\theta_2 - \theta_1) \dot{\theta}_1 \dot{\theta}_2 \quad (6.34)$$

Substituting equations (6.31), (6.33) and (6.34) in (6.30), one obtains the following:

$$\begin{aligned} M_2 &= (I_{2,A} + mL_2^2) \ddot{\theta}_2 + (m_2 L_1 r_{G_2} + mL_1 L_2) \cos(\theta_2 - \theta_1) \ddot{\theta}_1 \\ &\quad + (m_2 L_1 r_{G_2} + mL_1 L_2) \sin(\theta_2 - \theta_1) \dot{\theta}_1^2 \end{aligned} \quad (6.35)$$

## 7. SOLVING EQUATION OF MOTION FOR ACTUATOR TORQUES

The torque of actuator 1,  $M_1$ , is obtained by adding equations (6.29) and (6.35) as follows:

$$\begin{aligned}
 M_1 = & [I_{1,0} + (m_2 + m)L_1^2 + (m_2L_1r_{G_2} + mL_1L_2) \cos(\theta_2 - \theta_1)]\ddot{\theta}_1 \\
 & + [I_{2,A} + mL_2^2 + (m_2L_1r_{G_2} + mL_1L_2) \cos(\theta_2 - \theta_1)]\ddot{\theta}_2 \\
 & + (m_2L_1r_{G_2} + mL_1L_2) \sin(\theta_2 - \theta_1) \dot{\theta}_1^2 \\
 & - (m_2L_1r_{G_2} + mL_1L_2) \sin(\theta_2 - \theta_1) \dot{\theta}_2^2
 \end{aligned} \tag{7.1}$$

Similarly, the torque of actuator 2,  $M_2$ , is found by subtracting equation (6.29) from (6.35) and dividing each side of the resulting equation by 2 as follows:

$$\begin{aligned}
 M_2 = & \frac{1}{2} \{ [(m_2L_1r_{G_2} + mL_1L_2) \cos(\theta_2 - \theta_1) - I_{1,0} - (m_2 + m)L_1^2] \ddot{\theta}_1 \\
 & + [I_{2,A} + mL_2^2 - (m_2L_1r_{G_2} + mL_1L_2) \cos(\theta_2 - \theta_1)] \ddot{\theta}_2 \\
 & + (m_2L_1r_{G_2} + mL_1L_2) \sin(\theta_2 - \theta_1) \dot{\theta}_1^2 \\
 & + (m_2L_1r_{G_2} + mL_1L_2) \sin(\theta_2 - \theta_1) \dot{\theta}_2^2 \}
 \end{aligned} \tag{7.2}$$

## 8. CALCULATION OF ENERGY CONSUMPTION

The energy consumed during a complete operation is given by the following formula:

$$E = \int_{r_S}^{r_F} |\mathbf{M}_1 \cdot d\boldsymbol{\theta}_1| + |\mathbf{M}_2 \cdot (d\boldsymbol{\theta}_2 - d\boldsymbol{\theta}_1)| \quad (8.1)$$

where  $\mathbf{r}_S$  and  $\mathbf{r}_F$  denote the position vectors of the starting and final points of the trajectory, respectively. Explicitly expressed, these vectors are as follows:

$$\mathbf{r}_S = x_S \mathbf{i} + y_S \mathbf{j} \quad (8.2a)$$

$$\mathbf{r}_F = x_F \mathbf{i} + y_F \mathbf{j} \quad (8.2b)$$

It should be noted that the following requirements are to be satisfied:

$$x_S^2 + y_S^2 \leq (L_1 + L_2)^2 \quad (8.3a)$$

$$x_F^2 + y_F^2 \leq (L_1 + L_2)^2 \quad (8.3b)$$

Furthermore, the following relationship exists:

$$\mathbf{r}_F = \mathbf{r}_S + L \mathbf{u} \quad (8.4)$$

In terms of the components of position vectors  $\mathbf{r}_S$  and  $\mathbf{r}_F$ , equation (8.4) can be written as below:

$$x_F = x_S + L \cos \phi \quad (8.5a)$$

$$y_F = y_S + L \sin \phi \quad (8.5b)$$

The integral (8.1) can be calculated numerically after discretization of it.

## 9. NUMERICAL EXAMPLES

To carry out the computational procedure explained in Chapters 4-8, a MATLAB code was developed. This chapter is devoted to some numerical examples which help understand the solution approach presented in this work. It is assumed that actuators provide torques needed every time in the examples. Control dynamics is not considered. Masses and inertia moments of actuators are also omitted for simplicity. For all numerical examples, the manipulator is assumed to have the following physical parameters:

### Link 1:

$$L_1 = 0.4 \text{ m}$$

$$m_1 = 4 \text{ kg}$$

$$r_{G_1} = 0.5 L_1 = 0.2 \text{ m}$$

$$I_{G_1} = m_1 L_1^2 / 12 = 0.0533 \text{ kg-m}^2$$

$$I_{1,0} = I_{G_1} + m_1 r_{G_1}^2 = 0.2133 \text{ kg-m}^2$$

### Link 2:

$$L_2 = 0.2 \text{ m}$$

$$m_2 = 2 \text{ kg}$$

$$r_{G_2} = 0.5 L_2 = 0.1 \text{ m}$$

$$I_{G_2} = m_2 L_2^2 / 12 = 0.00167 \text{ kg-m}^2$$

### Payload:

$$m = 1 \text{ kg}$$

With these lengths of links, the length of longest possible trajectory becomes

$$L_{max} = 4\sqrt{L_1 L_2} = 4\sqrt{0.4 \times 0.2} = 1.1314 \text{ m}$$

In this chapter, five examples will be given for the following cases:

1.  $L = L_{max}$
2.  $L_{max}/2 < L < L_{max}$
3.  $L = L_{max}/2$
4.  $2L_2 < L < L_{max}/2$
5.  $L \leq 2L_2$

For each case, one numerical example is given. In each example, minimum values for cycloidal and 3-4-5 polynomial motion programs are calculated. Only figures of cycloidal motion program is provided since figures are very similar in both motion programs.

**Example 1:** ( $L = L_{max}$ )

Let  $L = L_{max}$  and  $T = 1$  second. As is known, there is only one solution to this case. Computer results are as follows:

$$x_{S_{init}} = x_{S_{fin}} = L_1 + L_2 = 0.6 \text{ m}$$

$$\varphi_{init} = \varphi_{fin} = 160.53^\circ$$

These values are common to the first and second configurations.

Minimum energy consumptions for the first configuration:

$$\min(EC_1) = 389.05 \text{ joules} \quad (\text{Cycloidal motion program})$$

$$\min(EC_1) = 344.77 \text{ joules} \quad (\text{3-4-5 polynomial motion program})$$

Minimum energy consumptions for the second configuration:

$$\min(EC_2) = 32.61 \text{ joules} \quad (\text{Cycloidal motion program})$$

$$\min(EC_2) = 29.37 \text{ joules} \quad (\text{3-4-5 polynomial motion program})$$

It is seen that the second configuration leads to the less consumption of energy for both motion programs. For each configuration of cycloidal motion program, how position coordinates, angular velocities, angular accelerations, actuator torques and actuator powers change versus time are shown in Figures 9.1-9.5 respectively.

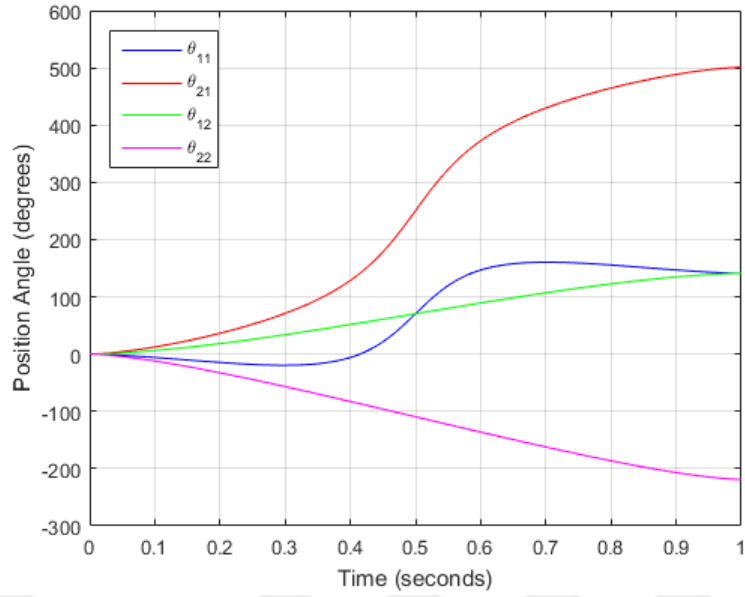


**Figure 9.1** Position angles of links in Example 1 ( $\theta_{11}$  and  $\theta_{21}$  are position angles of link 1 and link 2 for the first configuration while  $\theta_{12}$  and  $\theta_{22}$  are position angles of link 1 and link 2 for the second configuration)

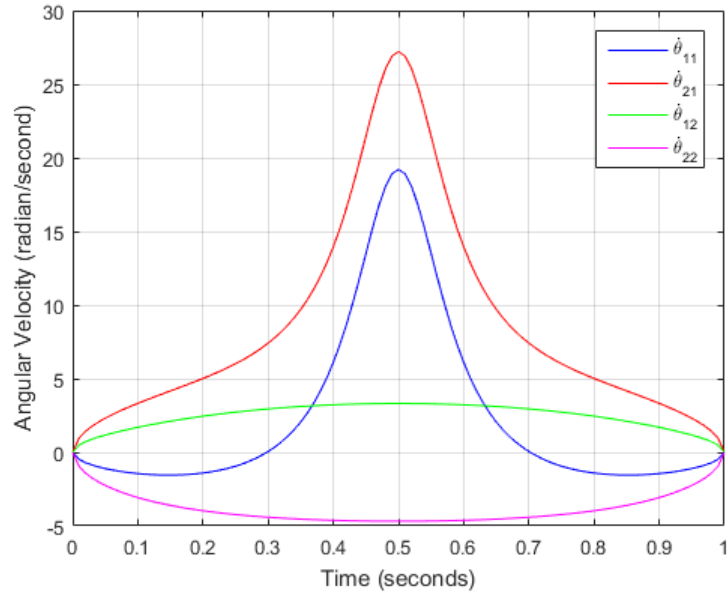


**Figure 9.2** Angular velocities of links in Example 1 ( $\dot{\theta}_{11}$  and  $\dot{\theta}_{21}$  are angular velocities of link 1 and link 2 for the first configuration while  $\dot{\theta}_{12}$  and  $\dot{\theta}_{22}$  are angular velocities of link 1 and link 2 for the second configuration)

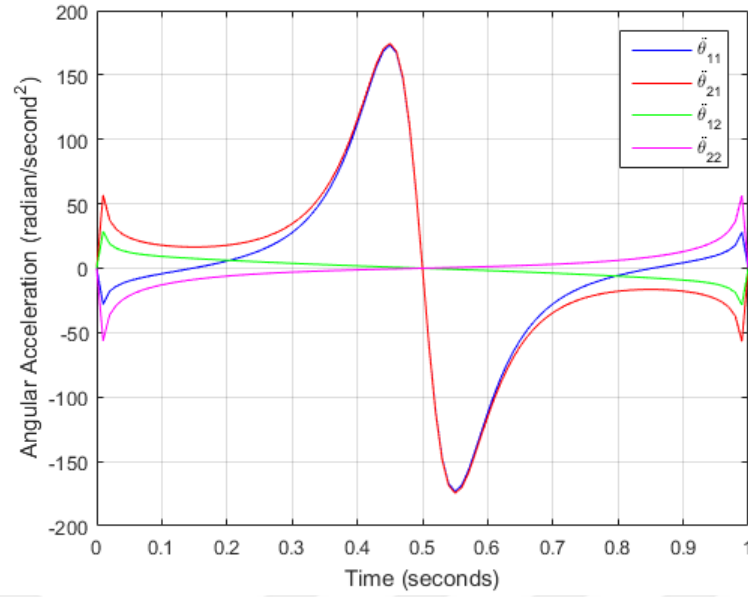


**Figure 9.3** Angular accelerations of links in Example 1 ( $\ddot{\theta}_{11}$  and  $\ddot{\theta}_{21}$  are angular accelerations of link 1 and link 2 for the first configuration while  $\ddot{\theta}_{12}$  and  $\ddot{\theta}_{22}$  are angular accelerations of link 1 and link 2 for the second configuration)

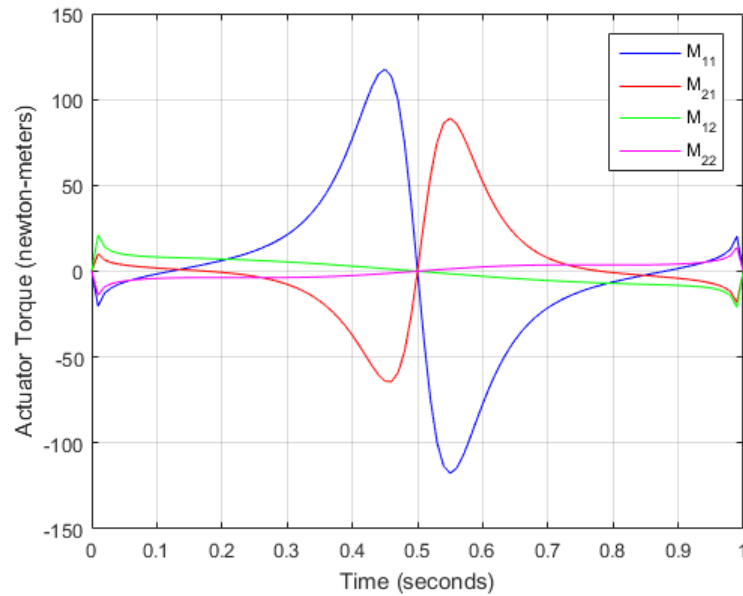


**Figure 9.4** Actuator torques of links in Example 1 ( $M_{11}$  and  $M_{21}$  are actuator torques of link 1 and link 2 for the first configuration while  $M_{12}$  and  $M_{22}$  are actuator torques of link 1 and link 2 for the second configuration)



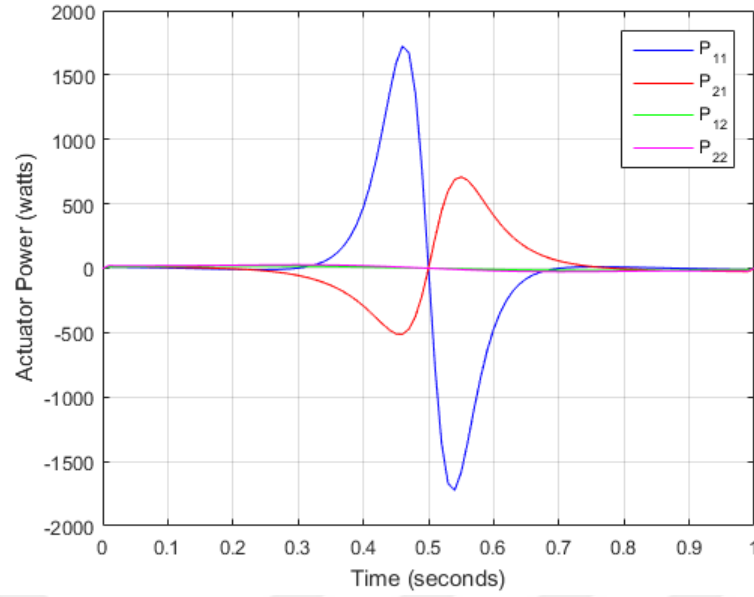


**Figure 9.5** Actuator powers of links in Example 1 ( $P_{11}$  and  $P_{21}$  are actuator powers of link 1 and link 2 for the first configuration while  $P_{12}$  and  $P_{22}$  are actuator powers of link 1 and link 2 for the second configuration)

**Example 2:** ( $L_{max}/2 < L < L_{max}$ )

Let  $L = 0.8 L_{max}$  and  $T = 1$  seconds.

Minimum energy consumptions for the first configuration:

$$\min(EC_1) = 36.24 \text{ joules} \quad (\text{Cycloidal motion program})$$

$$\min(EC_1) = 32.96 \text{ joules} \quad (\text{3-4-5 polynomial motion program})$$

For both motion programs, the abscissa of starting point and the direction angle of the optimal trajectories are same, hence, these two trajectories are identical:

$$x_{S,1} = L_1 + L_2 = 0.6 \text{ m}$$

$$\varphi_1 = \varphi_{init} = 138.96^\circ$$

Minimum energy consumptions for the second configuration:

$$\min(EC_2) = 16.54 \text{ joules} \quad (\text{Cycloidal motion program})$$

$$\min(EC_2) = 14.69 \text{ joules} \quad (\text{3-4-5 polynomial motion program})$$

Again, for both motion programs there exists only one trajectory. The abscissa of starting point and the direction angle of that trajectory are as follows:

$$x_{s,2} = 0.4764 \text{ m}$$

$$\varphi_2 = 155.18^\circ$$

Also for this case, the second configuration should be preferred regarding energy consumption.

Figures 9.6-9.10 depict the changes of positions, velocities, accelerations, torques and powers with respect to time. In Figure 9.11, we see how energy consumptions vary over direction angles.

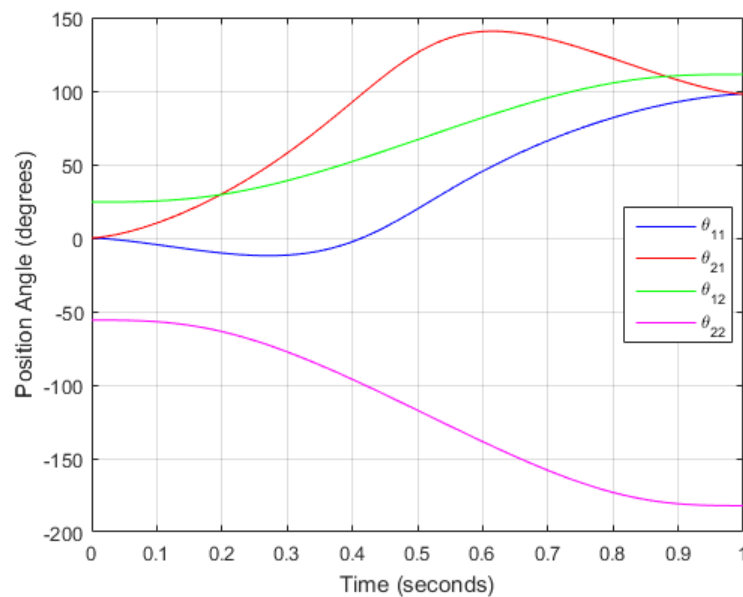


**Figure 9.6** Position angles of links in Example 2 ( $\theta_{11}$  and  $\theta_{21}$  are position angles of link 1 and link 2 for the first configuration while  $\theta_{12}$  and  $\theta_{22}$  are position angles of link 1 and link 2 for the second configuration)

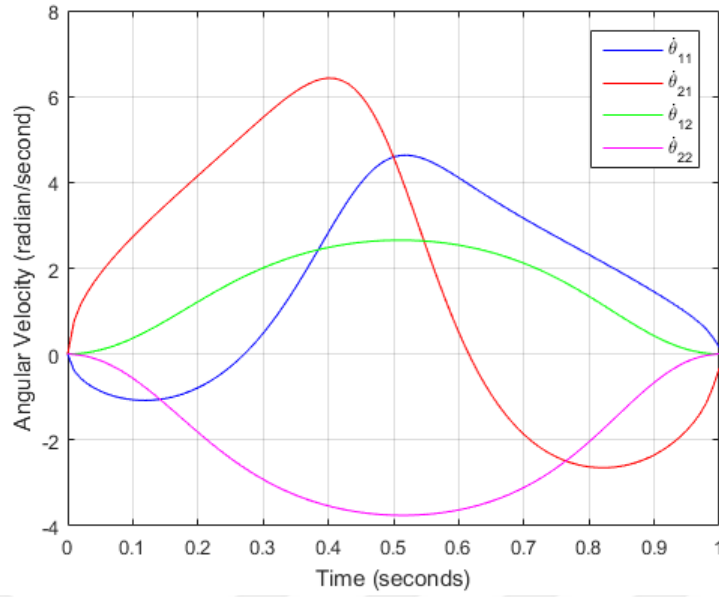


**Figure 9.7** Angular velocities of links in Example 2 ( $\dot{\theta}_{11}$  and  $\dot{\theta}_{21}$  are angular velocities of link 1 and link 2 for the first configuration while  $\dot{\theta}_{12}$  and  $\dot{\theta}_{22}$  are angular velocities of link 1 and link 2 for the second configuration)

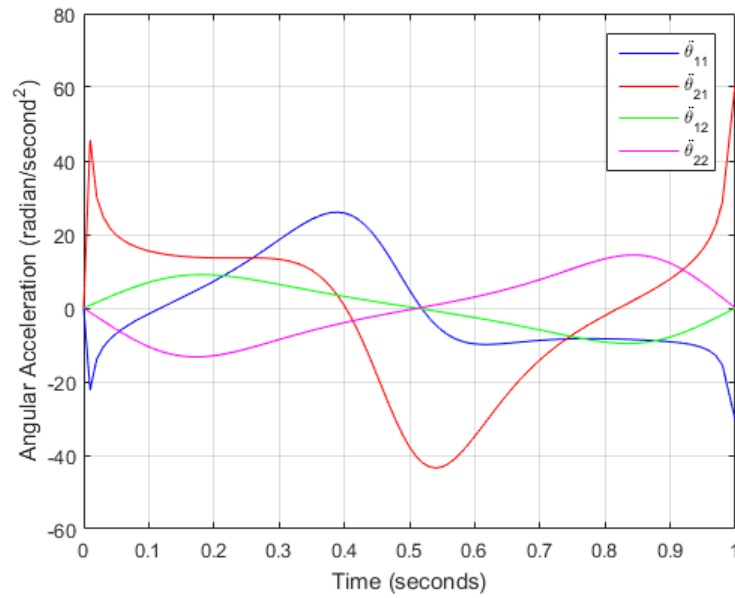


**Figure 9.8** Angular accelerations of links in Example 2 ( $\ddot{\theta}_{11}$  and  $\ddot{\theta}_{21}$  are angular accelerations of link 1 and link 2 for the first configuration while  $\ddot{\theta}_{12}$  and  $\ddot{\theta}_{22}$  are angular accelerations of link 1 and link 2 for the second configuration)

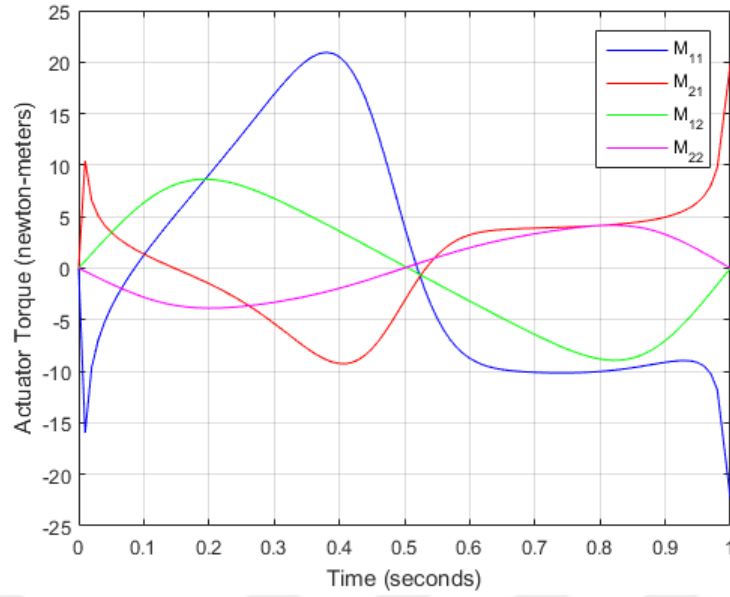


**Figure 9.9** Actuator torques of links in Example 2 ( $M_{11}$  and  $M_{21}$  are actuator torques of link 1 and link 2 for the first configuration while  $M_{12}$  and  $M_{22}$  are actuator torques of link 1 and link 2 for the second configuration)

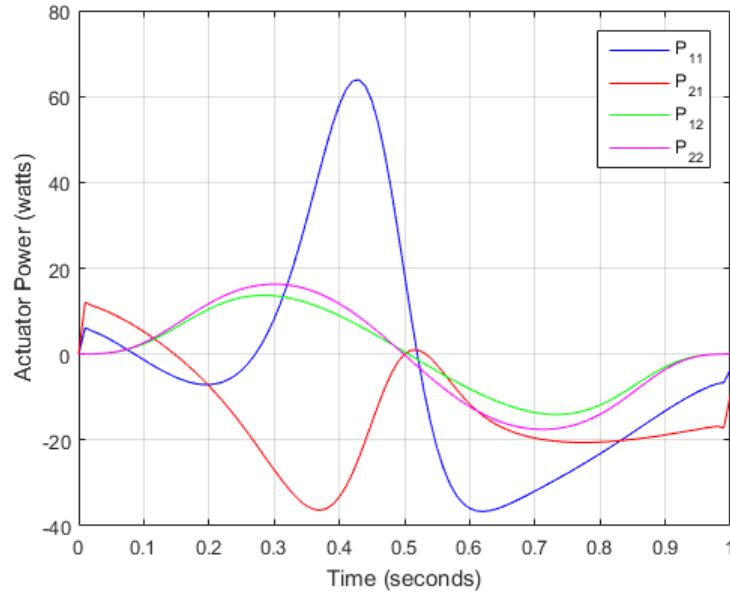


**Figure 9.10** Actuator powers of links in Example 2 ( $P_{11}$  and  $P_{21}$  are actuator powers of link 1 and link 2 for the first configuration while  $P_{12}$  and  $P_{22}$  are actuator powers of link 1 and link 2 for the second configuration)

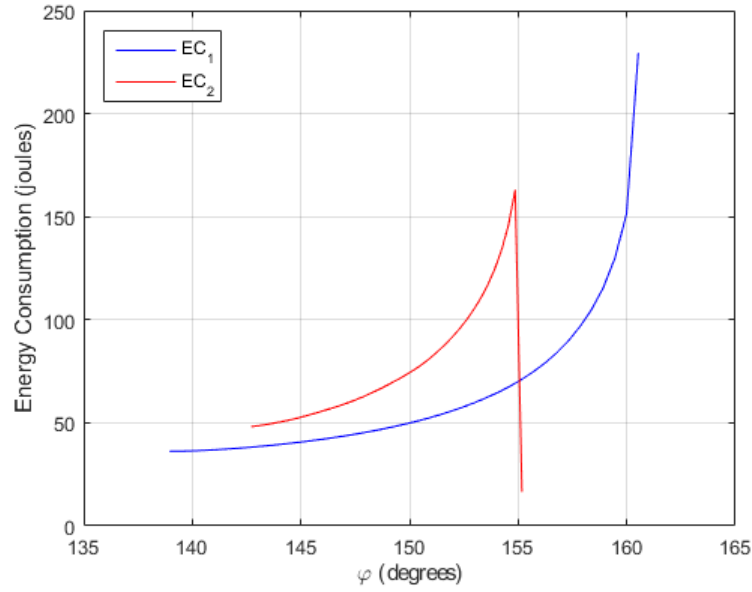


**Figure 9.11** Energy consumptions for both configurations in Example 2

**Example 3:** ( $L = L_{max}/2$ )

Let  $L = 0.5 L_{max}$  and  $T = 1$  seconds.

Minimum energy consumptions for the first configuration:

$$\min(EC_1) = 9.58 \text{ joules} \quad (\text{Cycloidal motion program})$$

$$\min(EC_1) = 8.48 \text{ joules} \quad (\text{3-4-5 polynomial motion program})$$

For both motion programs, energy-optimal trajectories are identical. The starting point and direction angle related to this trajectory are:

$$x_{s,1} = 0.52 \text{ m}$$

$$\varphi_1 = 121.92^\circ$$

Minimum energy consumptions for the second configuration:

$$\min(EC_2) = 5.53 \text{ joules} \quad (\text{Cycloidal motion program})$$

$$\min(EC_2) = 4.88 \text{ joules} \quad (\text{3-4-5 polynomial motion program})$$

Again, there is one energy-optimal trajectory common to both motion programs. Characteristic parameters related to this trajectory are:

$$x_{s,2} = 0.36 \text{ m}$$

$$\varphi_2 = 146.25^\circ$$

Figures 9.12-9.17 show the change of kinematic and kinetic parameters with time or direction angles.

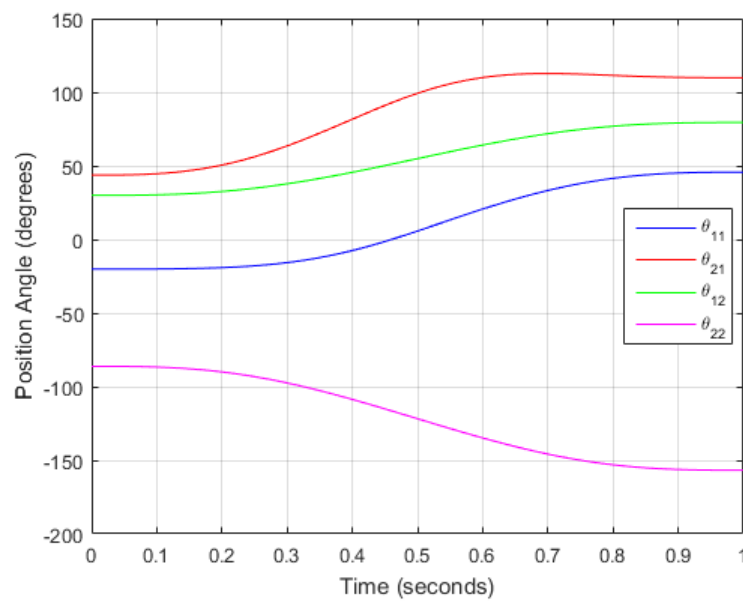


**Figure 9.12** Position angles of links in Example 3 ( $\theta_{11}$  and  $\theta_{21}$  are position angles of link 1 and link 2 for the first configuration while  $\theta_{12}$  and  $\theta_{22}$  are position angles of link 1 and link 2 for the second configuration)

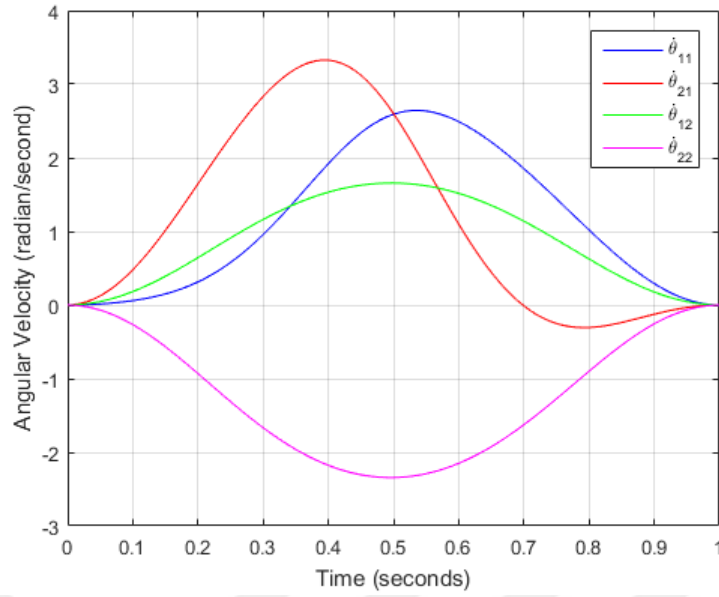


**Figure 9.13** Angular velocities of links in Example 3 ( $\dot{\theta}_{11}$  and  $\dot{\theta}_{21}$  are angular velocities of link 1 and link 2 for the first configuration while  $\dot{\theta}_{12}$  and  $\dot{\theta}_{22}$  are angular velocities of link 1 and link 2 for the second configuration)

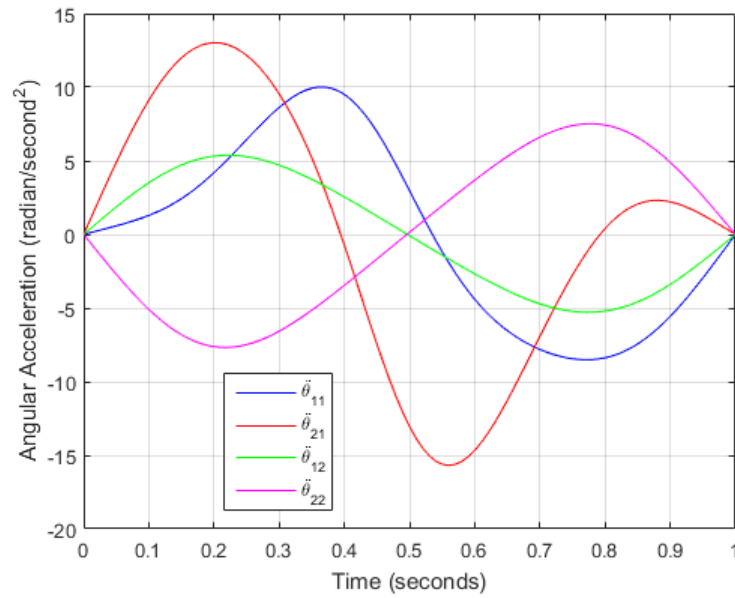


**Figure 9.14** Angular accelerations of links in Example 3 ( $\ddot{\theta}_{11}$  and  $\ddot{\theta}_{21}$  are angular accelerations of link 1 and link 2 for the first configuration as  $\ddot{\theta}_{12}$  and  $\ddot{\theta}_{22}$  are angular accelerations of link 1 and link 2 for the second configuration)

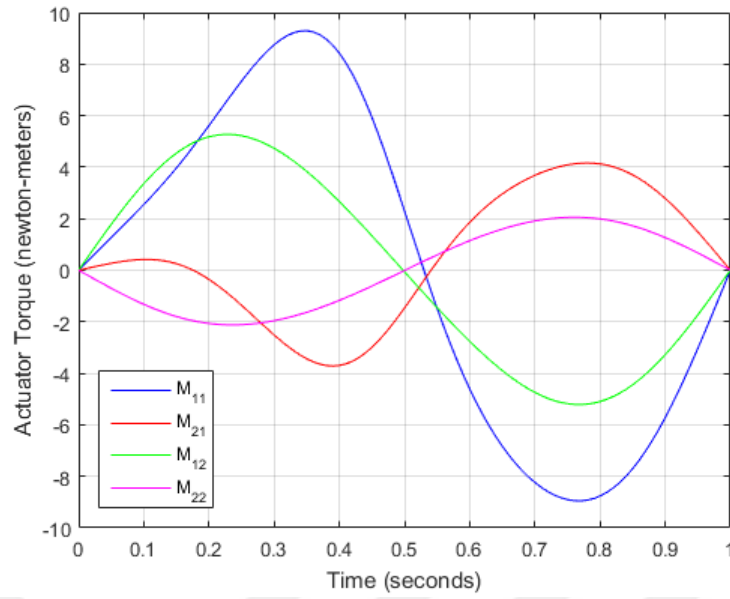


**Figure 9.15** Actuator torques of links in Example 3 ( $M_{11}$  and  $M_{21}$  are actuator torques of link 1 and link 2 for the first configuration while  $M_{12}$  and  $M_{22}$  are actuator torques of link 1 and link 2 for the second configuration)

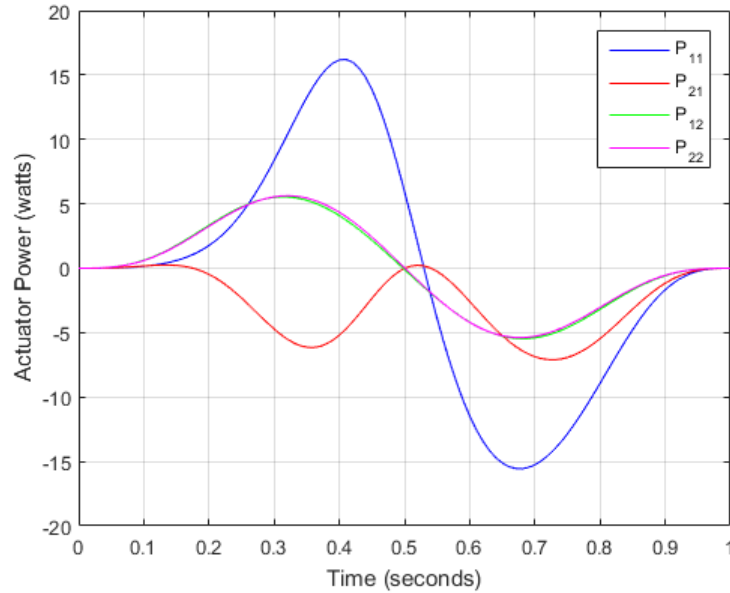


**Figure 9.16** Actuator powers of links in Example 3 ( $P_{11}$  and  $P_{21}$  are actuator powers of link 1 and link 2 for the first configuration while  $P_{12}$  and  $P_{22}$  are actuator powers of link 1 and link 2 for the second configuration)



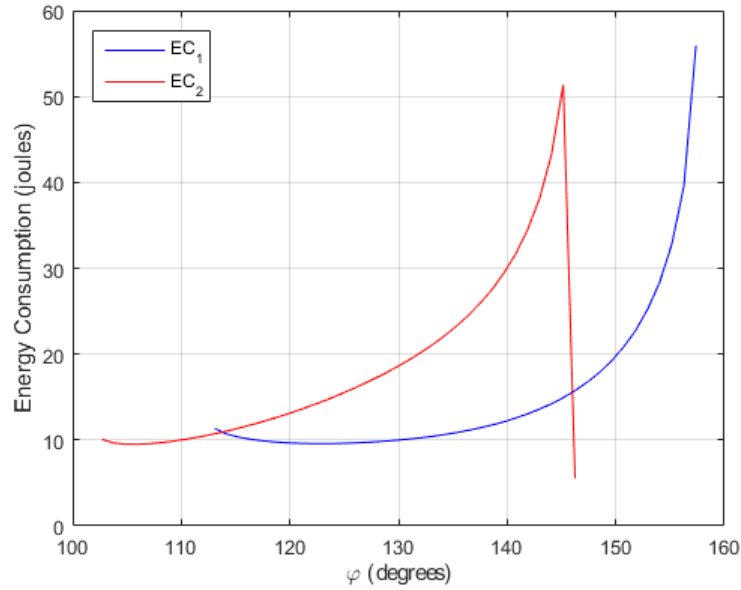


**Figure 9.17** Energy consumptions for both configurations in Example 3

**Example 4:** ( $2L_2 < L < L_{max}/2$ )

Let  $L = 0.4 L_{max}$  and  $T = 1$  seconds.

Minimum energy consumptions for the first configuration:

$$\min(EC_1) = 5.23 \text{ joules} \quad (\text{Cycloidal motion program})$$

$$\min(EC_1) = 4.63 \text{ joules} \quad (\text{3-4-5 polynomial motion program})$$

As in previous cases, energy-optimal trajectories are identical for both motion programs. The starting point and direction angle related to this trajectory are:

$$x_{s,1} = 0.52 \text{ m}$$

$$\varphi_1 = 130.89^\circ$$

Minimum energy consumptions for the second configuration:

$$\min(EC_2) = 3.44 \text{ joules} \quad (\text{Cycloidal motion program})$$

$$\min(EC_2) = 3.03 \text{ joules} \quad (\text{3-4-5 polynomial motion program})$$

The common energy-optimal trajectory has the following starting point and direction angle:

$$x_{s,2} = 0.28 \text{ m}$$

$$\varphi_2 = 134.42^\circ$$

The second configuration seems to be more economical also for this case. The relevant graphics are Figures 9.18-9.23.

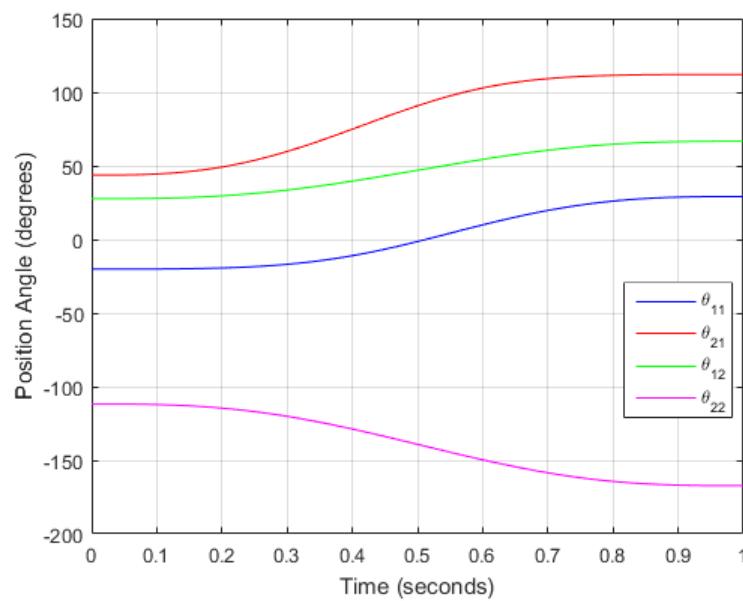


**Figure 9.18** Position angles of links in Example 4 ( $\theta_{11}$  and  $\theta_{21}$  are position angles of link 1 and link 2 for the first configuration while  $\theta_{12}$  and  $\theta_{22}$  are position angles of link 1 and link 2 for the second configuration)

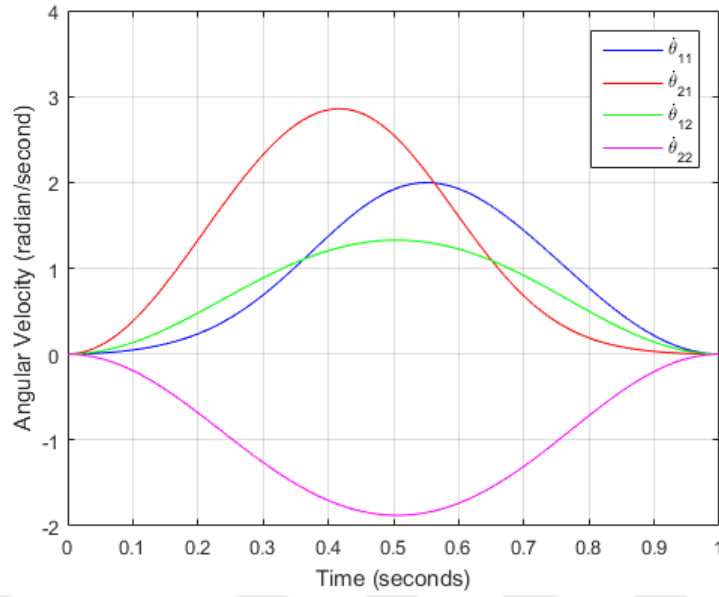


**Figure 9.19** Angular velocities of links in Example 4 ( $\dot{\theta}_{11}$  and  $\dot{\theta}_{21}$  are angular velocities of link 1 and link 2 for the first configuration while  $\dot{\theta}_{12}$  and  $\dot{\theta}_{22}$  are angular velocities of link 1 and link 2 for the second configuration)

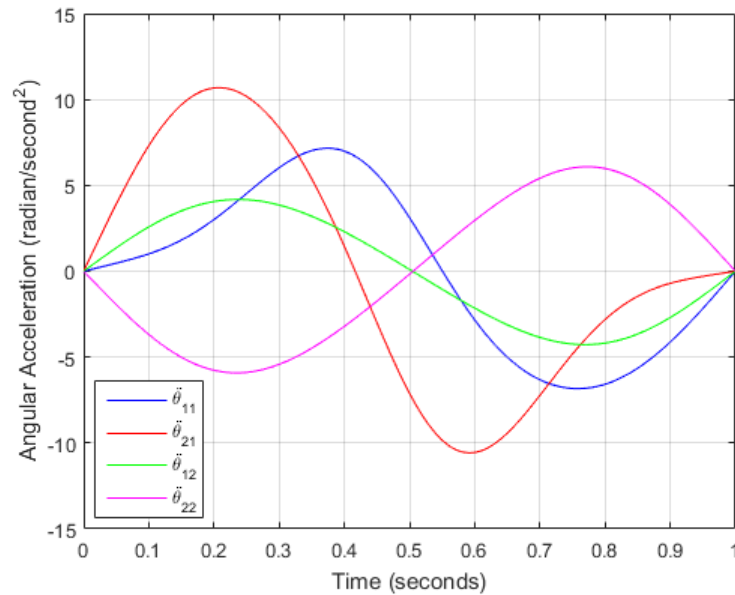


**Figure 9.20** Angular accelerations of links in Example 4 ( $\ddot{\theta}_{11}$  and  $\ddot{\theta}_{21}$  are angular accelerations of link 1 and link 2 for the first configuration as  $\ddot{\theta}_{12}$  and  $\ddot{\theta}_{22}$  are angular accelerations of link 1 and link 2 for the second configuration)

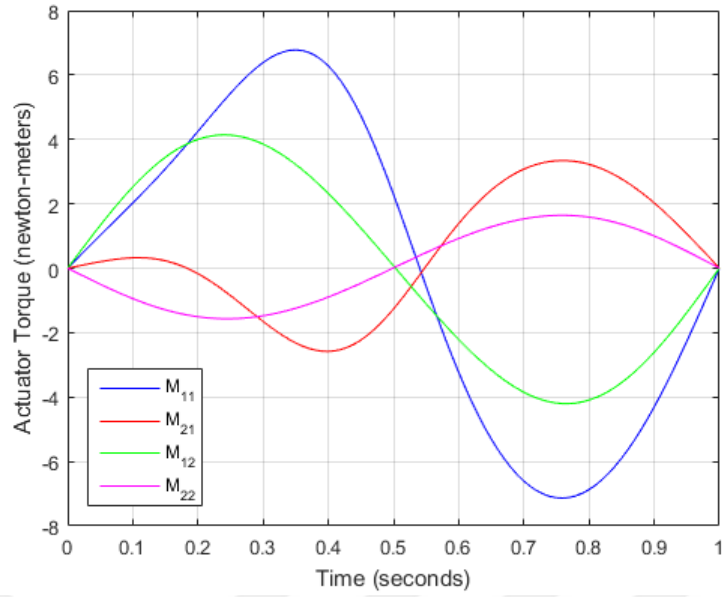


**Figure 9.21** Actuator torques of links in Example 4 ( $M_{11}$  and  $M_{21}$  are actuator torques of link 1 and link 2 for the first configuration while  $M_{12}$  and  $M_{22}$  are actuator torques of link 1 and link 2 for the second configuration)

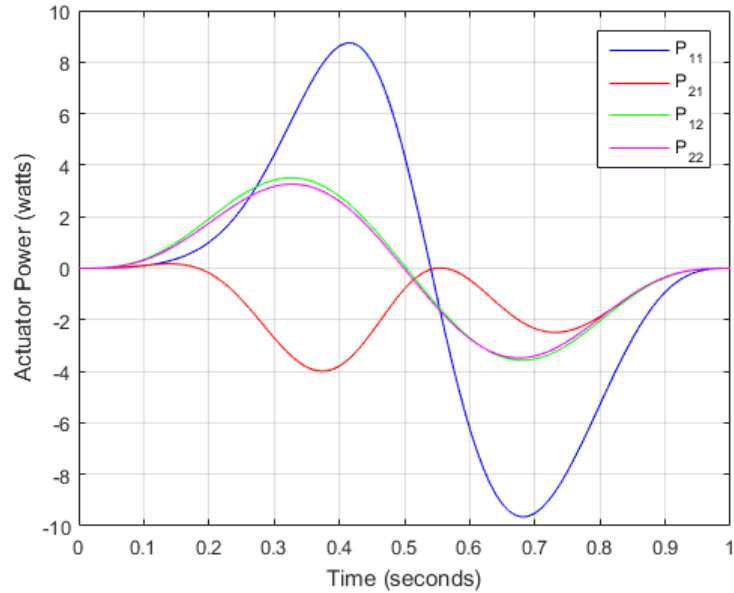


**Figure 9.22** Actuator powers of links in Example 4 ( $P_{11}$  and  $P_{21}$  are actuator powers of link 1 and link 2 for the first configuration while  $P_{12}$  and  $P_{22}$  are actuator powers of link 1 and link 2 for the second configuration)

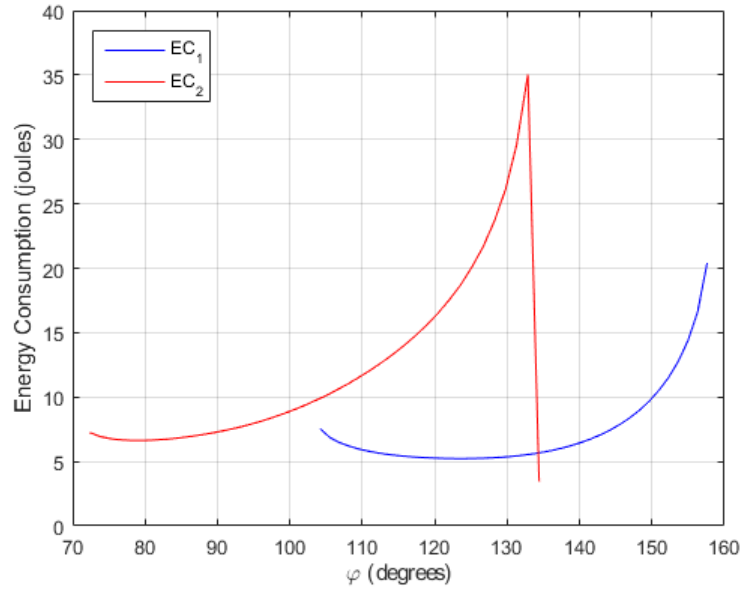


**Figure 9.23** Energy consumptions for both configurations in Example 4

**Example 5:** ( $L \leq 2L_2$ )

Let  $L = 0.2 L_{max}$  and  $T = 1$  seconds.

Minimum energy consumptions for the first configuration:

$$\min(EC_1) = 0.83 \text{ joules} \quad (\text{Cycloidal motion program})$$

$$\min(EC_1) = 0.74 \text{ joules} \quad (\text{3-4-5 polynomial motion program})$$

The common energy-optimal trajectory has the following characteristic values:

$$x_{S,1} = 0.52 \text{ m}$$

$$\varphi_1 = 130.3^\circ$$

Minimum energy consumptions for the second configuration:

$$\min(EC_2) = 0.59 \text{ joules} \quad (\text{Cycloidal motion program})$$

$$\min(EC_2) = 0.54 \text{ joules} \quad (\text{3-4-5 polynomial motion program})$$

For this configuration, the starting point's abscissa and the direction angle of the trajectory are as follows:

$$x_{s,2} = 0.44 \text{ m}$$

$$\varphi_2 = 67.19^\circ$$

The relevant graphics are presented in Figures 9.24-9.29.

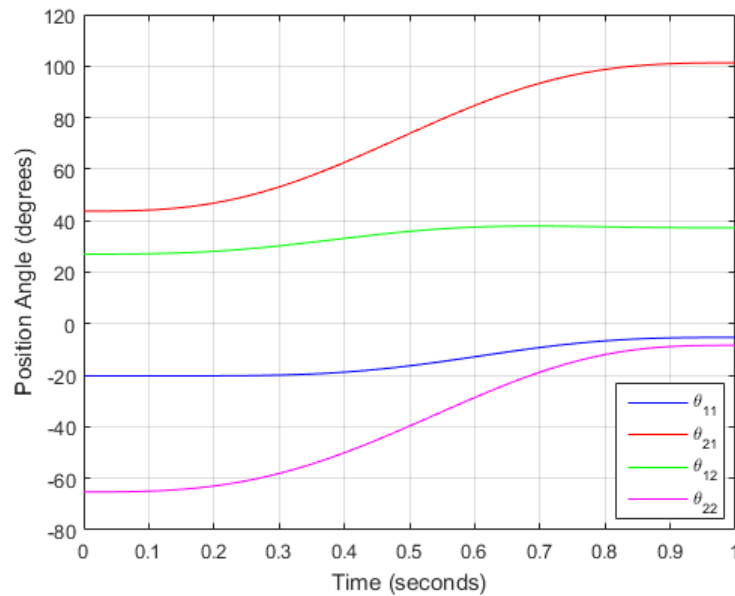


**Figure 9.24** Position angles of links in Example 5 ( $\theta_{11}$  and  $\theta_{21}$  are position angles of link 1 and link 2 for the first configuration while  $\theta_{12}$  and  $\theta_{22}$  are position angles of link 1 and link 2 for the second configuration)

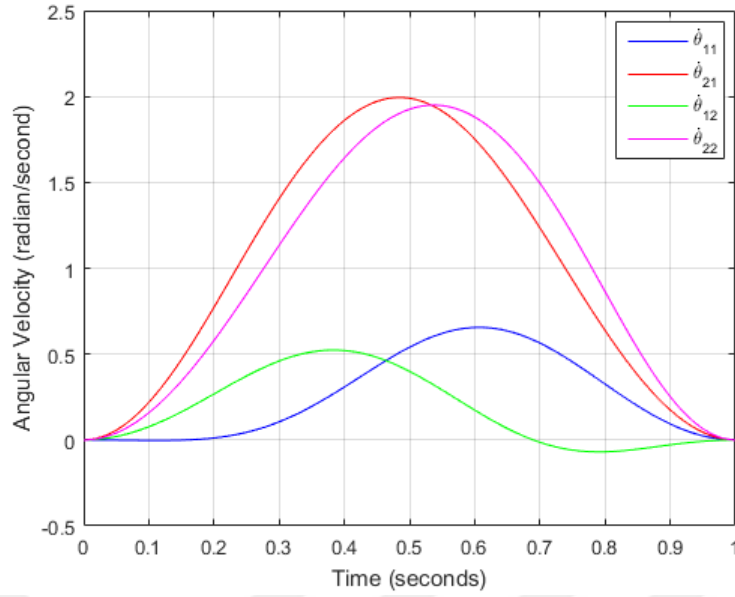


**Figure 9.25** Angular velocities of links in Example 5 ( $\dot{\theta}_{11}$  and  $\dot{\theta}_{21}$  are angular velocities of link 1 and link 2 for the first configuration while  $\dot{\theta}_{12}$  and  $\dot{\theta}_{22}$  are angular velocities of link 1 and link 2 for the second configuration)

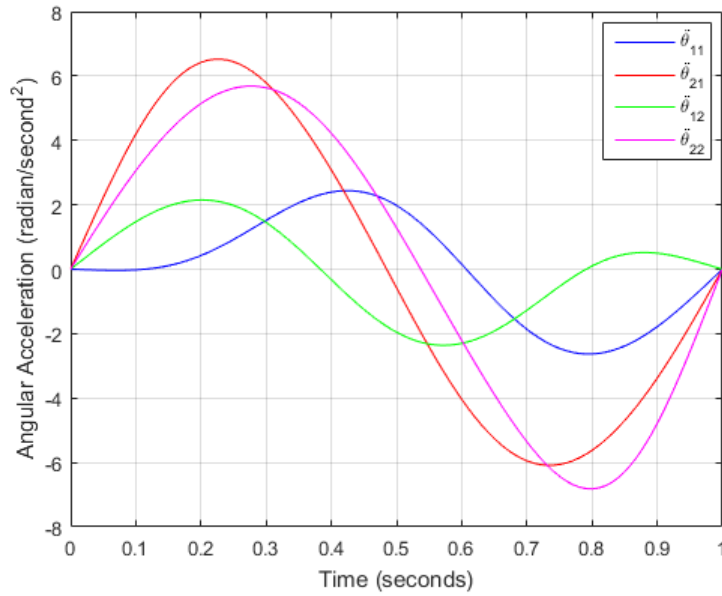


**Figure 9.26** Angular accelerations of links in Example 5 ( $\ddot{\theta}_{11}$  and  $\ddot{\theta}_{21}$  are angular accelerations of link 1 and link 2 for the first configuration as  $\ddot{\theta}_{12}$  and  $\ddot{\theta}_{22}$  are angular accelerations of link 1 and link 2 for the second configuration)

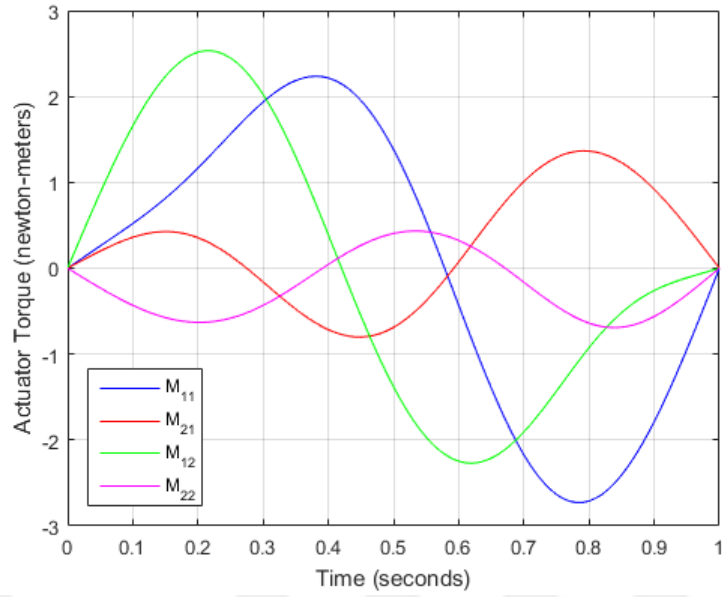


**Figure 9.27** Actuator torques of links in Example 5 ( $M_{11}$  and  $M_{21}$  are actuator torques of link 1 and link 2 for the first configuration while  $M_{12}$  and  $M_{22}$  are actuator torques of link 1 and link 2 for the second configuration)

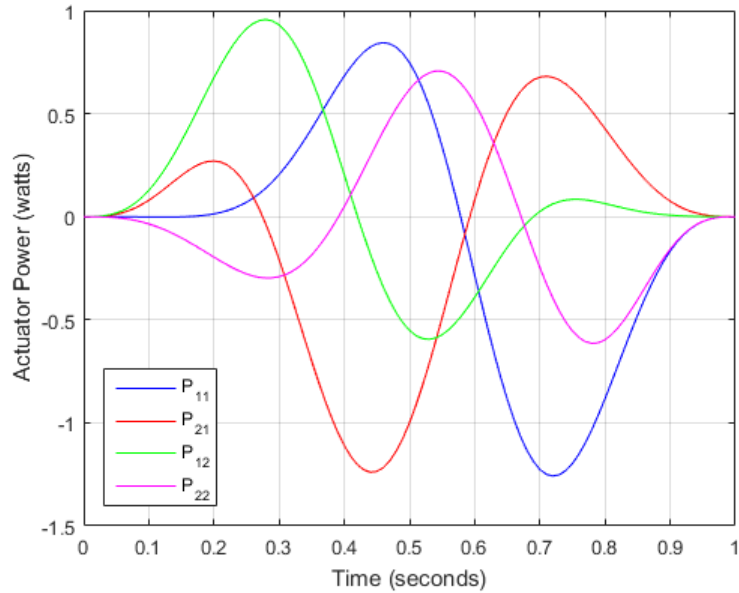


**Figure 9.28** Actuator powers of links in Example 5 ( $P_{11}$  and  $P_{21}$  are actuator powers of link 1 and link 2 for the first configuration while  $P_{12}$  and  $P_{22}$  are actuator powers of link 1 and link 2 for the second configuration)



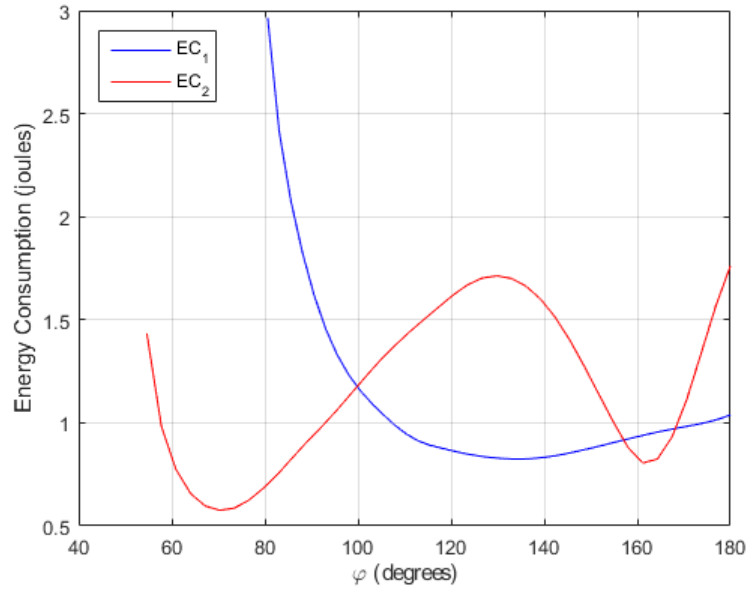


**Figure 9.29** Energy consumptions for both configurations in Example 5

For these five examples, the coordinates of the root of manipulator in the  $XY$ -coordinates fixed to the trajectories, provided that the starting points of all trajectories are coincided, are obtained as follows (Note that subscripts 1 and 2 refer to the first and second configurations and the relevant energy consumptions while superscripts denote the case number, see Ch. 4):

**The Coordinates of Root Location for Example 1:**

$${}^1X = {}^1X_1 = {}^1X_2 = -x_s \cos \varphi = -0.6 \cos(150.53^\circ) = 0.56 \text{ m}$$

$${}^1Y = {}^1Y_1 = {}^1Y_2 = x_s \sin \varphi = 0.6 \cos(160.53^\circ) = 0.1999 \text{ m}$$

**The Coordinates of Root Location for Example 2:**

$${}^2X_1 = -x_{s,1} \cos \varphi_1 = -0.6 \cos(138.96^\circ) = 0.4526 \text{ m}$$

$${}^2Y_1 = x_{s,1} \sin \varphi_1 = 0.6 \cos(138.96^\circ) = 0.3939 \text{ m}$$

$${}^2X_2 = -x_{s,2} \cos \varphi_2 = -0.4764 \cos(155.18^\circ) = -0.4324 \text{ m}$$

$${}^2Y_2 = x_{s,2} \sin \varphi_2 = 0.4764 \cos(155.18^\circ) = 0.1999 \text{ m}$$

**The Coordinates of Root Location for Example 3:**

$${}^3X_1 = -x_{S,1} \cos \varphi_1 = -0.52 \cos(121.92^\circ) = 0.2749 \text{ m}$$

$${}^3Y_1 = x_{S,1} \sin \varphi_1 = 0.52 \cos(121.92^\circ) = 0.4414 \text{ m}$$

$${}^3X_2 = -x_{S,2} \cos \varphi_2 = -0.36 \cos(146.25^\circ) = -0.2993 \text{ m}$$

$${}^3Y_2 = x_{S,2} \sin \varphi_2 = 0.36 \cos(146.25^\circ) = 0.2000 \text{ m}$$

**The Coordinates of Root Location for Example 4:**

$${}^4X_1 = -x_{S,1} \cos \varphi_1 = -0.52 \cos(130.89^\circ) = 0.3404 \text{ m}$$

$${}^4Y_1 = x_{S,1} \sin \varphi_1 = 0.52 \cos(130.89^\circ) = 0.3931 \text{ m}$$

$${}^4X_2 = -x_{S,2} \cos \varphi_2 = -0.28 \cos(134.42^\circ) = 0.1959 \text{ m}$$

$${}^4Y_2 = x_{S,2} \sin \varphi_2 = 0.28 \cos(134.42^\circ) = 0.1999 \text{ m}$$

**The Coordinates of Root Location for Example 5:**

$${}^5X_1 = -x_{S,1} \cos \varphi_1 = -0.52 \cos(130.3^\circ) = 0.3363 \text{ m}$$

$${}^5Y_1 = x_{S,1} \sin \varphi_1 = 0.52 \cos(130.3^\circ) = 0.3966 \text{ m}$$

$${}^5X_2 = -x_{S,2} \cos \varphi_2 = -0.44 \cos(67.19^\circ) = -0.1706 \text{ m}$$

$${}^5Y_2 = x_{S,2} \sin \varphi_2 = 0.44 \cos(67.19^\circ) = 0.4056 \text{ m}$$

These points are shown in Figure 9.30. Recall that, in this figure, the starting points of all trajectories are the origin of  $XY$ -coordinate system.

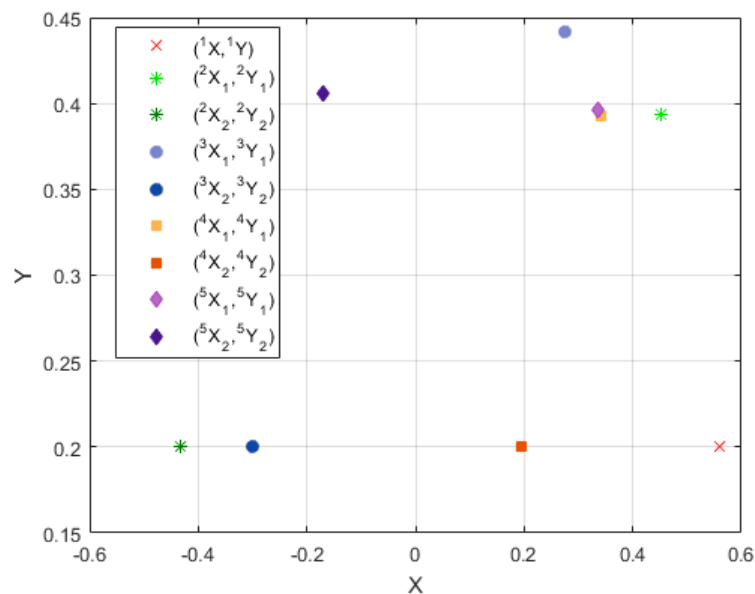


**Figure 9.30** The optimal loci of the root of manipulator in the  $XY$  coordinate system

## 10. CONCLUSION

The present study has focused on finding the optimal location of a 2-DoF manipulator, which makes the energy consumption minimum. To this end, two different motion programs were used: The cycloidal and the 3-4-5 polynomial motion programs. The common characteristics of these two motion programs are the smooth variation of their speed and acceleration functions.

Since it is assumed that  $L_1 > L_2$ , the manipulator considered has an annular workspace. In such a workspace, the maximum length that a trajectory in form of a straight-line can take is  $L_{max} = 4\sqrt{L_1L_2}$ . In regard to the length of trial trajectories, there are four different cases:  $L = L_{max}$ ,  $L_{max}/2 \leq L < L_{max}$ ,  $2L_2 < L < L_{max}/2$ ,  $L \leq 2L_2$ . For each case, there exists a range of abscissa of starting points. Similarly, for a trajectory length and its starting point given, the orientation angle varies between certain limits. Numerical results obviously demonstrate that a trajectory with minimal energy consumption can be found for each of four cases mentioned before.

The investigation of these energy-minimal trajectories was carried out in a coordinate system the origin of which is located at the root point of manipulator. However, when one wants to find the optimal location of the manipulator, another coordinate system in which the  $x$ -axis coincides with the direction of the energy-minimal trajectory must be used. In this thesis, actuators are assumed to provide necessary torques whenever needed, and their control is not considered. Consequently, future work can be focused on the control of actuators and extending the problem to 3D spatial robots.

## REFERENCES

- [1] Kopmaz O., Özcan R., Pala Y., The Determination of Trajectory in a 5R-1P Manipulator Using Regular Space Curves, *Proceedings of the ASME First European Joint Conference on System Design and Analysis*, **1992**, 1, 173-179.
- [2] Diken H., Energy Efficient Sinusoidal Path Planning of Robot Manipulator, *Journal of Mechanisms and Machine Theory*, **1994**, 29, 785-792.
- [3] Alshahrani S.A., Diken H., and Aljawi A.A.N., Optimum Trajectory Function for Minimum Energy Requirements of a Spherical Robot, *Proceedings of the 6th Saudi Engineering Conference*, **2002**, 4, 613-625.
- [4] Saramago S.F.P., Ceccarelli M., Effect of Basic Numerical Parameters on a Path Planning of Robots Taking into Account Actuating Energy, *Mechanism and Machine Theory*, **2004**, 39, 247-260.
- [5] Verscheuser D., Demeulenaere B., Swevers J., De Schutter J., Diehl M., Time-Energy Optimal Path Tracking for Robot: A Numerically Efficient Optimization Approach, *Robotics and Automation, ICRA '04 IEEE International Conference on Robotics and Automation Proceedings*, **2004**, 5, 4344-4349.
- [6] De Santos P.G., Garcia E., Ponticelli R., Armada M., Minimizing Energy Consumption in Hexapod Robots, *Advanced Robotics*, **2009**, 23, 681-704.
- [7] Chen C.-T., Liao T.-T., A Hybrid Strategy for the Time- and Energy-Efficient Trajectory Planning of Parallel Platform Manipulators, *Robotics and Computer-Integrated Manufacturing*, **2011**, 27, 72-81.
- [8] Gasparetto A., Boscaroli P., Lanzutti A., Vidoni R., Trajectory Planning in Robotics, *Mathematics in Computer Science*, **2012**, 6 (3), 269-279.
- [9] Gregory J., Olivares A., Staffetti E., Energy-Optimal Trajectory Planning for Robot Manipulators for Holonomic Constraints, *Systems & Control Letters*, **2012**, 61, 279-291.
- [10] Pellicciari M., Berselli G., Leali F., Vergnano A., A Method for Reducing the Energy Consumption of Pick-and-Place Industrial Robots, *Mechatronics*, **2013**, 23, 326-334.
- [11] Mohammed A., Schmidt B., Wang L., Gao L., Minimizing Energy Consumption for Robot Arm Movement, *Proceedings of the 8th International Conference on Digital Enterprise Technology*, **2014**, 25, 400-405.
- [12] Fung R.-F., Cheng Y.-H., Trajectory Planning Based on Minimum Absolute Input Energy for an LCD Glass-Handling Robot, *Applied Mathematical Modelling*, **2014**, 38, 2837-2847.
- [13] Paes K., Dewulf W., Vander Elst K., Kellens K., Slaets P., Energy Efficient Trajectories for an Industrial ABB Robot, *Proceedings of the 21st CIRP Conference on Life Cycle Engineering*, **2014**, 15, 105-110.

## **RESUME**

### **PERSONAL INFORMATION**

**Name and Surname** : Mehmet Beşir KOPMAZ  
**Birthdate and Place** : 7 February 1987, Bursa  
**Foreign Language** : English (Advanced), German (Beginner)  
**E-mail** : [mbkopmaz@gmail.com](mailto:mbkopmaz@gmail.com)

### **EDUCATIONAL STATUS**

<b>Degree</b>	<b>Department</b>	<b>University</b>	<b>Graduation</b>
B. Sc.	Computer Engineering	Boğaziçi University	June 2010

### **WORK EXPERIENCE**

<b>Year</b>	<b>Company</b>	<b>Position</b>
2014-...	Turk Telekom	IT Development Specialist
2011-2012	Turkish Airlines	Specialist

### **AWARDS**

1. Received scholarship from Kredi Yurtlar Kurumu for being in the first hundred participants in 2005 University Entrance Exam (2005-2010)